Rel-dependent decrease in the expression of ribosomal protein genes by inhibition of the respiratory electron transport chain in *Mycobacterium smegmatis*

Na-Kyeong Kim[1], Jong-Eun Baek[1], Ye-Jin Lee[1], Yuna Oh[1] and Jeong-Il Oh[1,2]*

[1]Department of Integrated Biological Science, Pusan National University, Busan, Republic of Korea,
[2]Microbiological Resource Research Institute, Pusan National University, Busan, Republic of Korea

In this study, we demonstrated that both the expression of most ribosomal protein genes and the amount of ribosomes were decreased in the Δaa_3 mutant of *Mycobacterium smegmatis*, in which the major terminal oxidase (aa_3 cytochrome *c* oxidase) of the respiratory electron transport chain (ETC) is inactivated, compared to those in the wild-type strain. Deletion of the *rel* gene encoding the major (p)ppGpp synthetase in the background of the Δaa_3 mutant restored the reduced expression of ribosomal protein genes, suggesting that inhibition of the respiratory ETC leads to the Rel-dependent stringent response (SR) in this bacterium. Both a decrease in the expression of ribosomal protein genes by overexpression of *rel* and the increased expression of *rel* in the Δaa_3 mutant relative to the wild-type strain support the Rel-dependent induction of SR in the Δaa_3 mutant. We also demonstrated that the expression of ribosomal protein genes was decreased in *M. smegmatis* exposed to respiration-inhibitory conditions, such as KCN and bedaquiline treatment, null mutation of the cytochrome bcc_1 complex, and hypoxia. The MprBA-SigE-SigB regulatory pathway was implicated in both the increased expression of *rel* and the decreased expression of ribosomal protein genes in the Δaa_3 mutant of *M. smegmatis*.

KEYWORDS

electron transport chain, MprBA two-component system, *Mycobacterium*, respiration, ribosome, SigB, SigE, stringent response

Introduction

Mycobacteria encounter a myriad of stress conditions, such as nutrient deprivation, hypoxia, and oxidative stress, when exposed to host environments (Bretl et al., 2011). The stringent response (SR) helps mycobacteria adapt to these hostile conditions by modulating their metabolism and redirecting resources toward functions that are beneficial to them under given conditions (Gupta et al., 2021). The SR is mediated by the secondary messenger molecules, guanosine tetraphosphate (ppGpp) and guanosine pentaphosphate (pppGpp) [collectively referred to as (p)ppGpp] (Bange et al., 2021). In

mycobacteria, SR has been suggested to affect survival under nutrient starvation, oxidative stress, and hypoxic conditions, as well as persistence, virulence, biofilm formation, cell division, cell morphology, and antibiotic tolerance, etc. (Primm et al., 2000; Betts et al., 2002; Dahl et al., 2003, 2005; Stallings et al., 2009; Klinkenberg et al., 2010; Weiss and Stallings, 2013; Gupta et al., 2016; Dutta et al., 2019). (p)ppGpp is produced by (p)ppGpp synthetase from the reactants ATP and GTP (or GDP). Two classes of (p)ppGpp synthetase occur in mycobacteria: the long Rel/SpoT homolog (RSH) and the small alarmone synthetase (SAS) (Prusa et al., 2018). The *Rv2583c* and *MSMEG_2965* genes encode the Rel proteins of the long RSH class in *Mycobacterium tuberculosis* and *Mycobacterium smegmatis*, respectively. Rel is a bifunctional enzyme with both (p)ppGpp synthetase and hydrolase activities and consists of an N-terminal catalytic domain with hydrolase/synthetase activities and a C-terminal regulatory domain (Avarbock et al., 1999, 2000, 2005; Primm et al., 2000; Singal et al., 2017; Bange et al., 2021). The C-terminal domain of Rel in mycobacteria harbors two subdomains: the "ThrRS, GTPase, and SpoT" (TGS) domain and "Aspartate kinase, Chorismate mutase and TyrA" (ACT) domain (Jain et al., 2006; Prusa et al., 2018; Bange et al., 2021; Shin et al., 2021a,b). *M. tuberculosis* and *M. smegmatis* have a single copy of the gene encoding SAS (*Rv1366* in *M. tuberculosis* and *MSMEG_5849* in *M. smegmatis*) (Murdeshwar and Chatterji, 2012; Weiss and Stallings, 2013). The Rv1366 protein was suggested to be catalytically inactive, while MSMEG_5849 annotated as RelZ was shown to be catalytically active and synthesize pGpp using GMP and ATP in addition to (p)ppGpp (Weiss and Stallings, 2013; Bag et al., 2014; Petchiappan et al., 2020). RelZ of *M. smegmatis* has been demonstrated to be a dual-domain SAS with the RNase HII and (p)ppGpp (pGpp) synthetase activities (Murdeshwar and Chatterji, 2012; Krishnan et al., 2016; Krishnan and Chatterji, 2020; Petchiappan et al., 2020). The expression of *relZ* was shown to be upregulated in *M. smegmatis* exposed to replication stress, such as UV stress (Krishnan et al., 2016), and the pGpp synthetase activity of RelZ was demonstrated to be inhibited by single-stranded RNA and pppGpp (Petchiappan et al., 2020).

The most prominent phenotypes of SR induction in bacteria are the downregulation of rRNA and ribosomal protein genes, along with the upregulation of amino acid biosynthesis genes (Prusa et al., 2018; Bange et al., 2021). In SR-induced mycobacteria, the expression of rRNA and ribosomal protein genes has been shown to be downregulated in a Rel-dependent manner (Dahl et al., 2003, 2005; Stallings et al., 2009; Prusa et al., 2018). In contrast, a RelZ-dependent decrease in the expression of rRNA and ribosomal protein genes has not been reported in mycobacteria. Currently, the role of RelZ is not certain, but based on its RNase HII activity, it has been suggested that RelZ plays a role in removing the R-loop during UV-induced replication stress (Krishnan et al., 2016).

Mycobacteria have the bifurcate respiratory electron transport chain (ETC) that is terminated with two terminal oxidases (Kana et al., 2001; Matsoso et al., 2005). One branch is terminated with the aa_3 cytochrome *c* oxidase, while the other is terminated with the *bd* quinol oxidase. The aa_3 cytochrome *c* oxidase forms a supercomplex with the cytochrome bcc_1 complex (Megehee et al.,

2006; Wiseman et al., 2018; Zhou et al., 2021). Since the aa_3 cytochrome *c* oxidase is the major terminal oxidase in *M. smegmatis* and *M. tuberculosis* grown aerobically, the bcc_1-aa_3 branch is required for optimal growth of the mycobacteria under aerobic conditions. Disruption of this branch results in growth impairment and upregulation of the *bd* quinol oxidase genes (Kana et al., 2001; Matsoso et al., 2005; Jeong et al., 2018; Beites et al., 2019; Ko and Oh, 2020). The *bd* quinol oxidase has been shown to have a high affinity for oxygen, thereby considered to play a crucial role under oxygen-limiting conditions and when the aa_3 cytochrome *c* oxidase is inactivated (Puustinen et al., 1991; Kana et al., 2001; Belevich et al., 2007).

The MprBA two-component system (TCS), consisting of the membrane-bound MprB histidine kinase and its cognate MprA response regulator, was initially found to be necessary for *M. tuberculosis* to cause persistent infection (Zahrt and Deretic, 2001; Zahrt, 2003). In *M. tuberculosis* and *M. smegmatis*, the MprBA TCS has been found to be activated upon exposure to surface stress and alkaline pH (He et al., 2006; Pang et al., 2007; White et al., 2010). Besides ATP, inorganic polyphosphate synthesized by polyphosphate kinase was found to serve as a phosphate donor for MprB-mediated MprA phosphorylation (Sureka et al., 2007). The MprBA-SigE-Rel regulatory pathway has been suggested to be implicated in induction of (p)ppGpp synthesis and SR in mycobacteria (Sureka et al., 2007; Sanyal et al., 2013). In *M. tuberculosis* and *M. smegmatis*, the phosphorylated MprA positively regulates the expression of *sigE*, and the alternative sigma factor SigE in turn binds to the promoter of *rel* to activate its transcription (He et al., 2006; Sureka et al., 2007). Recently, we reported that the SigE-SigB regulatory pathway is activated in an aa_3 oxidase mutant of *M. smegmatis* grown aerobically relative to the isogenic wild-type (WT) strain grown under the same conditions (Oh et al., 2022). This finding suggests the possibility that SR could be induced in *M. smegmatis* under respiration-inhibitory conditions. In this study, we demonstrate that SR is indeed induced in *M. smegmatis* through the MprBA-SigE-SigB-Rel signaling pathway when the respiratory ETC is inhibited.

Materials and methods

Bacterial strains, plasmids, and culture conditions

The bacterial strains and plasmids used in this study are listed in Table 1. *Escherichia coli* strains were grown in Lysogeny Broth (LB) medium at 37°C. *M. smegmatis* strains were grown in Middlebrook 7H9 medium (Difco, Sparks, MD, United States) supplemented with 0.2% (w/v) glucose (7H9-glucose) and 0.02% (v/v) Tween 80 as an anti-clumping agent at 37°C. For glucose-limiting conditions, *M. smegmatis* strains were grown aerobically in 7H9 medium supplemented with 0.01% (w/v) glucose and 0.02% (v/v) Tween 80. For hypoxic growth of *M. smegmatis* strains, a 100-ml flask was filled with 80 mL of aerobically grown culture with an optical density at 600 nm (OD_{600}) of 0.7–0.75 and tightly sealed with a rubber stopper. The culture was incubated on a gyratory shaker for 3 h at 37°C, allowing for a gradual depletion of O_2 from the growth medium. For

TABLE 1 Strains and plasmids used in this study.

Strain/plasmid	Relevant phenotype/genotype*	Reference
Strains		
E. coli DH5α	φ80d*lacZ*ΔM15 Δ*lacU169 recA1 endA1 hsdR17 supE44 thi1 gyrA96 relA1*	Jessee (1986)
M. smegmatis mc²155	High-transformation-efficiency mutant of *M. smegmatis* ATCC 607	Snapper et al. (1990)
M. smegmatis Δ*sigE*	*MSMEG_5072* (*sigE*) deletion mutant of *M. smegmatis* mc²155	Oh et al. (2022)
M. smegmatis Δ*sigB*	*MSMEG_2752* (*sigB*) deletion mutant of *M. smegmatis* mc²155	Oh et al. (2022)
M. smegmatis Δ*aa₃*	*MSMEG_4268* (*ctaC*) deletion mutant of *M. smegmatis* mc²155	Jeong et al. (2018)
M. smegmatis Δ*mprA*	*MSMEG_5488* (*mprA*) deletion mutant of *M. smegmatis* mc²155	This study
M. smegmatis Δ*rel*	*MSMEG_2965* (*rel*) deletion mutant of *M. smegmatis* mc²155	This study
M. smegmatis Δ*bc₁*	*MSMEG_4263* (*qcrB*) deletion mutant of *M. smegmatis* mc²155	This study
M. smegmatis Δ*aa₃*Δ*sigE*	*MSMEG_4268* (*ctaC*) and *MSMEG_5072* (*sigE*) double-deletion mutant of *M. smegmatis* mc²155	Oh et al. (2022)
M. smegmatis Δ*aa₃*Δ*sigB*	*MSMEG_4268* (*ctaC*) and *MSMEG_2752* (*sigB*) double-deletion mutant of *M. smegmatis* mc²155	Oh et al. (2022)
M. smegmatis Δ*aa₃*Δ*mprA*	*MSMEG_4268* (*ctaC*) and *MSMEG_5488* (*mprA*) double-deletion mutant of *M. smegmatis* mc²155	This study
M. smegmatis Δ*aa₃*Δ*rel*	*MSMEG_4268* (*ctaC*) and *MSMEG_2965* (*rel*) double-deletion mutant of *M. smegmatis* mc²155	This study
Plasmids		
pNC	Hygʳ; promoterless *lacZ*	Oh et al. (2010)
pNCII	Hygʳ; a derivative of pNC, the ribosome-binding site of *lacZ* is removed (translational fusion)	Oh et al. (2020)
pMH201	Kmʳ; acetamide-inducible promoter, derivative of pMV306	Kang et al. (2005)
pKOTs	Hygʳ; pKO-based vector constructed by inserting HindIII-KpnI fragment containing pAL500Ts and the pUC ori derived from pDE	Jeong et al. (2013)
pMV306	Kmʳ; integration vector containing the *int* and *attP* sites of mycobacteriophage L5 for integration into the mycobacterial genome	Stover et al. (1991)
pUC19	Ampʳ; *lacPOZ'*	Yanisch-Perron et al. (1985)
pNCIIrel	pNCII::0.436-kb XbaI-ClaI fragment containing the *MSMEG_2965* (*rel*) promoter region	This study
pNCIIeis	pNCII::0.508-kb XbaI-BamHI fragment containing the *Rv2416c* (*eis*) promoter region	This study
pNCIIwag31	pNCII::0.490-kb XbaI-ClaI fragment containing the *Rv2145c* (*wag31*) promoter region	This study
pUC19mprA	pUC19::1.472-kb HindIII-EcoRV fragment containing *mprA* of *M. smegmatis*	This study
pUC19Δ*mprA*	pUC19::1.337-kb HindIII-EcoRV fragment containing Δ*mprA*	This study
pKOTsΔ*mprA*	pKOTs::1.337-kb HindIII-EcoRV fragment from pUC19Δ*mprA*	This study
pKOTsΔ*rel*	pKOTs::0.736-kb NotI-HindIII fragment containing Δ*rel*	This study
pKOTsΔ*bc₁*	pKOTs::0.818-kb NotI-HindIII fragment containing Δ*bc₁*	This study
pMH201rel	pMV306::2.417-kb NdeI-ClaI fragment containing C-terminally His-tagged *MSMEG_2965* (*rel*)	This study
pMV306ctaC	pMV306::1.37-kb XbaI-HindIII fragment containing *MSMEG_4268* (*ctaC*)	Jeong et al. (2018)

*Abbreviations: Ampʳ, ampicillin resistance; Hygʳ, hygromycin resistance; Kmʳ, kanamycin resistance.

treatment of *M. smegmatis* cultures with potassium cyanide (KCN), *M. smegmatis* strains were grown until the OD$_{600}$ reached 0.45–0.5. Following the addition of KCN to the cultures to a final concentration of 50 μM, the cultures were further grown for 2 h. Ampicillin (100 μg/mL for *E. coli*), kanamycin (50 μg/mL for *E. coli* and 30 μg/mL for *M. smegmatis*), and hygromycin (200 μg/mL for *E. coli* and 50 μg/mL for *M. smegmatis*) were added to the growth medium when required.

DNA manipulation and electroporation

Standard protocols and manufacturers' instructions were followed for recombinant DNA manipulations (Green and Sambrook, 2012). Transformation of *M. smegmatis* with plasmids was carried out by electroporation as described elsewhere (Snapper et al., 1990). The primers used for PCR are listed in Table 2.

Construction of plasmids

The temperature-sensitive suicide plasmids for the construction of mutant strains of *M. smegmatis*

To construct pKOTsΔrel, we performed two rounds of recombination PCR. Using the chromosomal DNA of *M. smegmatis* as a template, two primary PCR reactions were conducted. The first reaction utilized the primers F_relmut and R_relrec, while the second used the primers F_relrec and R_relmut, resulting in two 38-bp

TABLE 2 Oligonucleotides used in this study.

Oligonucleotide	Nucleotide sequences (5′ → 3′)	Purpose
F_mprAmut	ATATAAGCTTGTGCAATCGTCGCCGTCG	Δ*mprA* construction
R_mprAmut	GTTCGCCGGAGATGACGTC	Δ*mprA* construction
F_relmut	ATTTGCGGCCGCCGTGCAGTCTCCTCCC	Δ*rel* construction
R_relmut	ATTTAAGCTTGCCGCATCCACGCCATGTC	Δ*rel* construction
F_relrec	CATGGACACCACCACGCTGGTCAAGGGCCGCGACTTCG	Δ*rel* construction
R_relrec	CGAAGTCGCGGCCCTTGACCAGCGTGGTGGTGTCCATG	Δ*rel* construction
F_bc1mut	ATTAGCGGCCGCGTCATCACCTTCCTCATGG	Δ*bc*₁ construction
R_bc1mut	ATTAAAGCTTGGGAGTGGCGCATATAGAAAG	Δ*bc*₁ construction
F_bc1rec	CTTCTGCTGCTGATCGGTTACGTCGAGCTGCACCAG	Δ*bc*₁ construction
R_bc1rec	CTGGTGCAGCTCGACGTAACCGATCAGCAGCAGAAG	Δ*bc*₁ construction
F_rellacZII	ATATTCTAGACTGGATGCGCGCGGTTTC	*rel*::*lacZ* translational fusion
R_rellacZII	ATATATCGATAGACTGCACGGCCTGACC	*rel*::*lacZ* translational fusion
F_eislacZII	ATATTCTAGACCAAGGCATGGTTGGGCAC	*eis*::*lacZ* translational fusion
R_eislacZII	ATATGGATCCCGGGCTACACAGGGTCACAGTC	*eis*::*lacZ* translational fusion
F_wag31lacZII	ATATTCTAGACCGTGACTGGCGTCCCAC	*wag31*::*lacZ* translational fusion
R_wag31lacZII	ATATATCGATGGCAGGTGTAAGCGGCATTGT	*wag31*::*lacZ* translational fusion
F_rel_His	ATTTCATATGGTCGACGAGCCAGGC	*rel* overexpression
R_rel_His	ATTTATCGATTCAGTGATGGTGATGGTGATGGGCCGCGCTGGTGACGCG	*rel* overexpression
F_sigA_RT	CTTGAGGTGACCGACGATCT	qRT-PCR
R_sigA_RT	AGCTTCTTCTTCCTCGTCCT	qRT-PCR
F_cydA_RT	CGGTGGCAGTTCGGAATCAC	qRT-PCR
R_cydA_RT	CAGAAAAAGTTTGCCGAAGAAACG	qRT-PCR
F_1441_RT	AAGGTGATCGCGAGCGCTG	qRT-PCR
R_1441_RT	GGAAGGCACGGCCCTGGG	qRT-PCR
F_1470_RT	TCGCAGAGCCCATCTCGGTC	qRT-PCR
R_1470_RT	GCGTGTACCCCTCGGTGACAC	qRT-PCR
F_1525_RT	GGGTCGTCCTCGCACCAG	qRT-PCR
R_1525_RT	GTTGTGCAGAGCACCCTTCTTGG	qRT-PCR
F_2654_RT	GCCGAGCAGAAAAAAGAGATCCTG	qRT-PCR
R_2654_RT	GCGACGTACTTCAGCAGGCG	qRT-PCR
F_6894_RT	CGTCGCCTCCCGTGGGG	qRT-PCR
R_6894_RT	CGTTGACCGACAGCGTGACAT	qRT-PCR

overlapping DNA fragments (401 and 384 bp, respectively). Both PCR products contain the same 540-bp deletion within *rel* in the overlapping region. In the secondary PCR, a 747-bp DNA fragment with a deletion in the *rel* gene was obtained using both the primary PCR products as templates, along with the primers F_relmut and R_relmut. The resulting secondary PCR product was restricted with NotI and HindIII and subsequently cloned into pKOTs, resulting in pKOTsΔrel.

To construct pKOTsΔmprA, a PCR reaction was carried out with the primers F_mprAmut and R_mprAmut using the chromosomal DNA of *M. smegmatis* as a template. The resulting 1,469-bp DNA fragment, encompassing the 406-bp upstream and 374-bp downstream regions of *mprA*, was digested with HindIII. Subsequently, the restricted PCR product was cloned into pUC19 that had been digested with SmaI and HindIII, resulting in pUC19mprA. A 135-bp DNA fragment within *mprA* was removed from pUC19mprA using XhoI. The linear plasmid was self-ligated through the XhoI recognition site, yielding pUC19ΔmprA. Using pUC19ΔmprA as a template, another PCR reaction was performed with the primers F_mprAmut and R_mprAmut, resulting in a 1,343-bp DNA fragment with a deletion in *mprA*. The obtained PCR product was then restricted with HindIII and cloned into pKOTs that had been digested with HindIII and EcoRV, resulting in pKOTsΔmprA.

To construct pKOTsΔbc$_1$, we performed two rounds of recombination PCR. We used the chromosomal DNA of *M. smegmatis* as a template for two primary PCR reactions. The first reaction was performed with the primers F_ bc1mut and R_ bc1rec, while the second used the primers F_bc1rec and R_ bc1mut, resulting in two 36-bp overlapping DNA fragments (481 and 384 bp, respectively). Both PCR products contain the same 1,309-bp deletion within *qcrB* in the overlapping region. In the secondary PCR, an 829-bp DNA fragment with a deletion in *qcrB* was obtained using both the primary PCR products as templates, along with the primers F_bc1mut and R_bc1mut. The secondary PCR product was restricted with NotI and HindIII, and cloned into pKOTs, yielding pKOTsΔbc$_1$.

pNCIIrel, pNCIIeis, and pNCIIwag31

The plasmid pNCIIrel is a *rel::lacZ* translational fusion plasmid that contains the 5′ portion (39 bp) of *rel* and the 397-bp DNA sequence upstream of *rel*. For the construction of pNCIIrel, a 456-bp DNA fragment was amplified using the chromosomal DNA of *M. smegmatis* as a template and the primers F_rellacZII and R_rellacZII. The PCR product was restricted with XbaI and ClaI and cloned into the promoterless *lacZ* vector pNCII, yielding pNCIIrel.

The plasmid pNCIIeis is an *eis::lacZ* translational fusion plasmid that contains the 5′ portion (24 bp) of *eis* and the 474-bp DNA sequence upstream of *eis*. To construct pNCIIeis, a 518-bp DNA fragment was amplified using the chromosomal DNA of *M. tuberculosis* as a template and the primers F_eislacZII and R_eislacZII. The PCR product was restricted with XbaI and BamHI and cloned into pNCII, yielding pNCIIeis.

The plasmid pNCIIwag31 is a *wag31::lacZ* translational fusion plasmid that contains the 5′ portion (18 bp) of *wag31* and the 463-bp DNA sequence upstream of *wag31*. To construct pNCIIwag31, a 501-bp DNA fragment was amplified using the chromosomal DNA of *M. tuberculosis* as a template and the primers F_wag31lacZII and R_wag31lacZII. The PCR product was restricted with XbaI and ClaI and cloned into pNCII, creating pNCIIwag31.

pMH201rel

The plasmid pMH201rel is a derivative of the pMH201 integration vector that contains the C-terminally His$_6$-tagged *rel* gene. A 2,429-bp DNA fragment encompassing the *rel* gene and six His codons immediately before its stop codon was amplified by PCR with the primers F_rel_His and R_rel_His, using the chromosomal DNA of *M. smegmatis* as a template. The PCR product was restricted with NdeI and ClaI and cloned into pMH201 with an acetamide-inducible promoter, yielding pMH201rel.

Construction of mutant strains of *M. smegmatis*

The Δ*rel*, Δ*aa$_3$*Δ*rel*, Δ*mprA*, Δ*aa$_3$*Δ*mprA*, and Δ*bc$_1$* deletion mutants of *M. smegmatis* were generated through allelic exchange mutagenesis, which utilized the corresponding pKOTs-derived suicide plasmids (pKOTsΔrel, pKOTsΔmprA, and pKOTsΔbc$_1$). The mutagenesis was performed in the background of the WT or Δ*aa$_3$* mutant strain, following the procedure previously described (Jeong et al., 2013). In brief, the temperature-sensitive suicide plasmid was introduced into *M. smegmatis* by electroporation. Transformants were selected at 30°C (replication-permissive temperature) on 7H9-glucose agar plates containing hygromycin, and the selected transformants were grown in 7H9-glucose liquid medium supplemented with hygromycin for 3 days at 30°C. Heterogenotes of *M. smegmatis*, which were generated by a single recombination event, were selected for their hygromycin resistance on 7H9-glucose agar plates at 42°C (replication-non-permissive temperature). The selected heterogenotes were grown on 7H9-glucose medium without antibiotics for 3 days at 37°C. Isogenic homogenates were obtained from the heterogenotes after a second recombination by selecting them for sucrose resistance on 7H9-glucose agar plates containing 10% (w/v) sucrose at 37°C. The allelic exchange was verified by PCR using isolated genomic DNA.

RNA sequencing analysis

Three biological replicate cultures of the Δ*aa$_3$*, Δ*aa$_3$*Δ*rel*, and Δ*aa$_3$*Δ*mprA* strains were grown aerobically to OD$_{600}$ of 0.45–0.5. Total RNA of each culture was isolated as described previously (Kim et al., 2010). rRNA was eliminated from the isolated total RNA using the NEBNext rRNA Depletion kit (Bacteria) (NEB, Ipswich, MA, United States). The RNA sequencing libraries were created using a TruSeq standard mRNA Sample Prep Kit (Illumina, San Diego, CA, United States). The libraries were quantified using a KAPA Library Quantification Kit (KAPA Biosystems, Wilmington, MA, United States) for Illumina Sequencing platforms according to the qPCR Quantification Protocol Guide and qualified using the TapeStation D1000 ScreenTape (Agilent, Santa Clara, CA, United States). Indexed libraries were subsequently submitted to an Illumina NovaSeq (Illumina), and the paired-end (2×101 bp) sequencing of the nine libraries was conducted on an Illumina NovaSeq 6,000 platform at Macrogen Inc. (Seoul, South Korea) using the NovaSeq 6,000 sequencing protocol (Illumina). Paired-end reads (101 bp) were then mapped to the reference genome sequence of *M. smegmatis* mc^{2}155 (GCF_000015005.1_ASM1500v1) with the program Bowtie 1.1.2 using default settings. Based on principal component analysis of the gene expression patterns in the *M. smegmatis*

strains, one result from each of the Δaa_3, $\Delta aa_3\Delta rel$, and $\Delta aa_3\Delta mprA$ strains was considered as an outlier and therefore excluded from subsequent analyses. The RNA sequencing data for the Δaa_3, $\Delta aa_3\Delta rel$, and $\Delta aa_3\Delta mprA$ strains of *M. smegmatis* were deposited in NCBI's Gene Expression Omnibus and are accessible through the GEO Series accession number GSE267048.

The RNA sequencing data for the WT and Δaa_3 strains of *M. smegmatis* strains have been previously deposited in NCBI's Gene Expression Omnibus with the GEO Series accession number GSE155251 (Oh et al., 2020).

β-galactosidase assay and determination of the protein concentration

The β-galactosidase activity was measured spectrophotometrically as described previously (Oh and Kaplan, 1999). The protein concentration was determined using a Bio-Rad protein assay kit (Bio-Rad, Hercules, CA, United States) with bovine serum albumin as the standard protein.

Quantitative real-time PCR

RNA isolation from *M. smegmatis* strains and cDNA synthesis were performed as described elsewhere (Kim et al., 2010), with the exception of using a random hexamer primer (Thermo Fisher Scientific, Waltham, MA, United States) in place of gene-specific primers in cDNA synthesis. The presence of DNA contamination in the isolated RNA was assessed through PCR using the primers intended for use in quantitative real-time PCR (qRT-PCR). To determine the transcript levels of *MSMEG_1441, MSMEG_1470, MSMEG_1525, MSMEG_2654, MSMEG_6894, cydA* and *sigA*, qRT-PCR was performed in a 20-µl mixture. The mixture contained 5 µL of the template cDNA, 1 µL (15 pmol) of each of two gene-specific primers, 10 µL of TB GreenTM Premix Ex TaqTM (Tli RNase Plus) (Takara, Tokyo, Japan), 0.4 µL of the ROX passive fluorescent dye, and 2.6 µL of distilled water. The thermal cycling process commenced with 1 cycle at 95°C for 2 min, followed by 40 cycles of 95°C for 5 s and 64°C for 30 s. The *sigA* gene, which encodes the principal sigma factor, was employed as a reference gene for qRT-PCR to normalize the expression levels of *MSMEG_1441, MSMEG_1470, MSMEG_1525, MSMEG_2654, MSMEG_6894*, and *cydA*. Melting curve analysis was conducted for each reaction to verify the amplification of a single PCR product during qRT-PCR. The primers used for qRT-PCR are listed in Table 2.

Western blotting analysis

Cell-free crude extracts were subjected to SDS-PAGE, and proteins on the gel were transferred to polyvinylidene fluoride membranes (Millipore, Burlington, MA, United States). Western blotting was performed as described previously (Mouncey and Kaplan, 1998). For detection of His$_6$-tagged Rel, a mouse monoclonal IgG against His$_6$ (Thermo Fisher Scientific; MA1-21315) was used at a 1:2,000 dilution. A horseradish peroxidase (HRP)-conjugated anti-mouse IgG (Bio-Rad) was used at a 1:10,000 for the detection of the primary antibody. The ECL kit (Advansta, San Jose, CA, United States) was used to visualize protein bands via a ChemiDoc imaging system (Bio-Rad).

Ribosome profiling using sucrose density gradient sedimentation

The WT and Δaa_3 strains of *M. smegmatis* were grown aerobically to an OD$_{600}$ of 0.45 to 0.5 in 50 mL of 7H9-glucose medium. After harvesting the bacterial cells by centrifugation, the cell pellets were washed with 1 mL of BP buffer [20 mM Tris–HCl (pH 7.5), 10 mM MgCl$_2$, 100 mM NH$_4$Cl, and 5 mM β-mercaptoethanol] and then resuspended in 0.5 mL of BP buffer. Cells were broken three times using a Fastprep FP120 (Thermo Fisher Scientific), and cell-free lysates were obtained by centrifugation at $12,000 \times g$, for 15 min at 4°C. Then, 0.5 mL of cleared lysates from the WT and Δaa_3 strains, with their OD$_{260}$ values adjusted to be identical, were added to 10 mL of a 5–40% sucrose gradient in BP buffer and resolved by ultracentrifugation at 4°C in a Beckman SW41 rotor for 2.5 h at 37,000 rpm. The sucrose density gradient solution was eluted from the bottom of the centrifuge tube, and the presence of polysomes, ribosomes, and ribosomal subunits was monitored at 254 nm. The amounts of polysomes, assembled 70S ribosomes, and ribosomal subunits were compared between the WT and Δaa_3 strains after normalizing the ribosome profiles to the absorbance of ultraviolet (UV: 254 nm)-absorbing fractions containing proteins, nucleic acids, nucleotides, and other components.
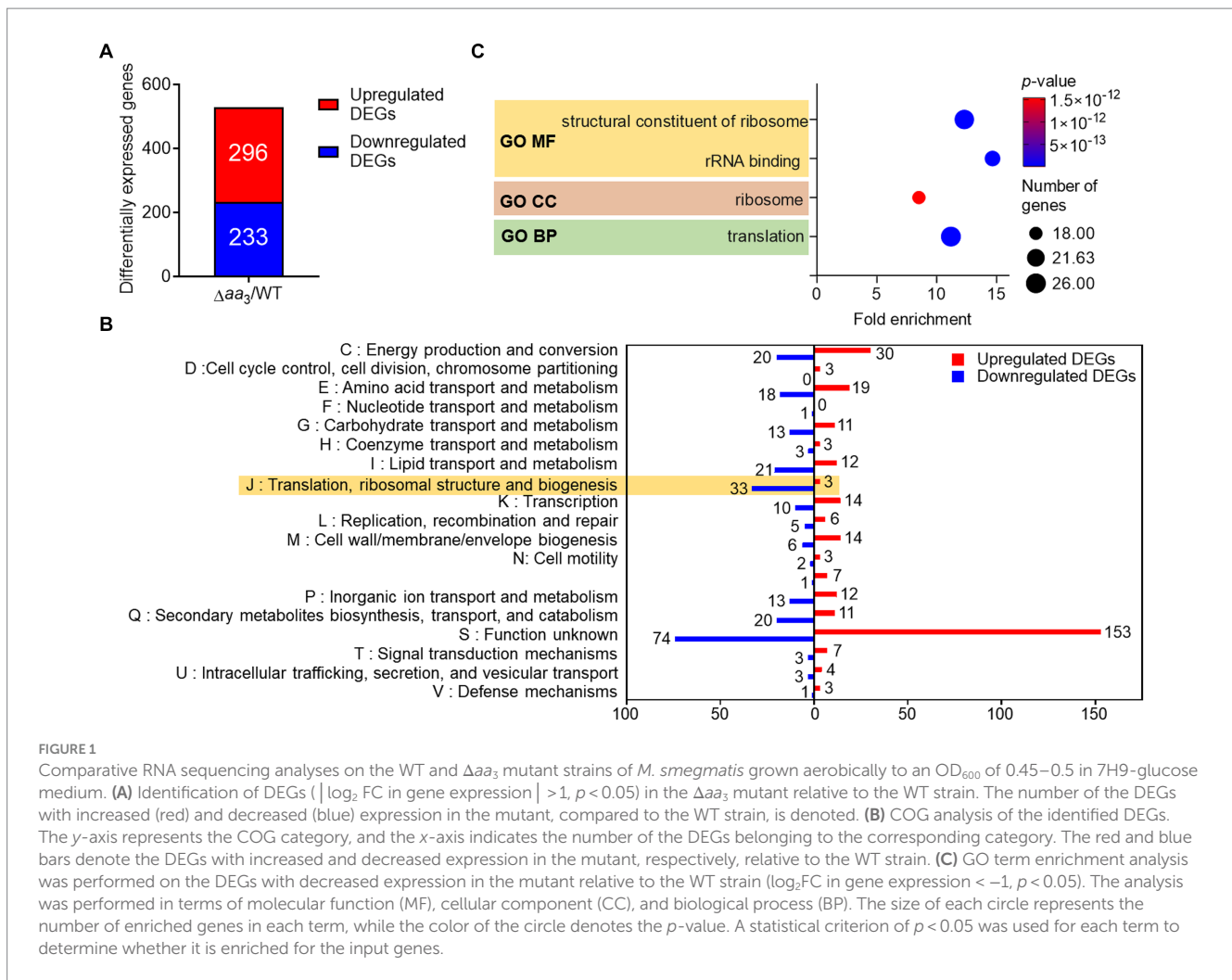
Statistical analysis

Results were subjected to statistical analysis using GraphPad Prism 10.0 (GraphPad software Inc., La Jolla, CA, United States). At least three biological replicates were used for each experiment. The data were evaluated statistically using an unpaired Student t-test. Differences were considered statistically significant at $p < 0.05$.

Results

Induction of SR under conditions that inhibit the respiratory ETC

M. tuberculosis in granulomas encounters conditions inhibiting the respiration ETC, such as hypoxia, nutrient deprivation, nitrosative stress, and low pH, etc. (Timm et al., 2003; Baker and Abramovitch, 2018). These conditions have been considered signals for *M. tuberculosis* to transition into a dormant state. To gain insights into metabolic and physiological changes in mycobacteria exposed to conditions inhibiting the respiratory ETC, we performed comparative RNA sequencing analysis on the WT strain of *M. smegmatis* and its isogenic Δaa_3 mutant strain with a deletion in the *ctaC* gene encoding subunit II of the aa_3 cytochrome *c* oxidase (Oh et al., 2020). The Δaa_3 mutant strain has an impaired growth rate and 50% respiration inhibition compared to the WT strain (Jeong et al., 2018). As shown in Figure 1A, we identified 529 differentially expressed genes (DEGs) whose expression was altered in the Δaa_3 mutant strain by more than |log$_2$ fold change (FC)| > 1 with a p-value less than 0.05 relative to the WT strain (Supplementary Table S1). Among the identified DEGs, 296 were upregulated and 233 were downregulated in the Δaa_3 mutant relative to the WT strain. We carried out clusters of orthologous group (COG) analysis with the identified DEGs to gain insights into changes in the Δaa_3 mutant strain. The COG analysis

FIGURE 1

Comparative RNA sequencing analyses on the WT and Δaa_3 mutant strains of *M. smegmatis* grown aerobically to an OD_{600} of 0.45−0.5 in 7H9-glucose medium. **(A)** Identification of DEGs (│log₂ FC in gene expression│ >1, $p < 0.05$) in the Δaa_3 mutant relative to the WT strain. The number of the DEGs with increased (red) and decreased (blue) expression in the mutant, compared to the WT strain, is denoted. **(B)** COG analysis of the identified DEGs. The *y*-axis represents the COG category, and the *x*-axis indicates the number of the DEGs belonging to the corresponding category. The red and blue bars denote the DEGs with increased and decreased expression in the mutant, respectively, relative to the WT strain. **(C)** GO term enrichment analysis was performed on the DEGs with decreased expression in the mutant relative to the WT strain (log₂FC in gene expression < −1, $p < 0.05$). The analysis was performed in terms of molecular function (MF), cellular component (CC), and biological process (BP). The size of each circle represents the number of enriched genes in each term, while the color of the circle denotes the *p*-value. A statistical criterion of $p < 0.05$ was used for each term to determine whether it is enriched for the input genes.

was conducted based on eggNOG v5.0[1] (Huerta-Cepas et al., 2019) (Figure 1B). Except for the "S" category representing function unknown, the "J" category exhibited the largest number of DEGs with the reduced expression in the Δaa_3 mutant relative to the WT strain. The "J" category encompasses genes related to translation, ribosomal structure and biogenesis. The second-largest number of downregulated DEGs belonged to the "I" category consisting of genes related to lipid transport and metabolism. Excluding the "S" category, the largest number of DEGs with the increased expression in the mutant relative to the WT strain belonged to the "C" category, which is associated with energy production and conversion.

To gain further insights into the functions associated with DEGs downregulated in the Δaa_3 mutant compared to the WT strain, enrichment of gene ontology (GO) in terms of molecular function (MF), cellular component (CC), and biological process (BP) was assessed using the DAVID functional annotation tool[2] (Huang da et al., 2009; Sherman et al., 2022) (Figure 1C). Genes related to translation and ribosomes, such as ribosomal protein genes, were statistically significantly enriched

in three GO terms. The decreased expression of genes related to ribosomes and translation is a representative phenomenon of SR (Prusa et al., 2018; Bange et al., 2021), suggesting the possibility of SR induction in *M. smegmatis* under conditions that inhibit the respiratory ETC.

We compared the relative expression levels of a total of 56 genes encoding the ribosomal proteins using the RNA sequencing data from the WT vs. Δaa_3 strains. As shown in Figure 2A, the expression of most ribosomal protein genes was downregulated in the Δaa_3 mutant strain relative to the WT strain. To examine whether the decreased expression of the ribosomal protein genes in the Δaa_3 mutant is due to the Rel-dependent induction of SR, we compared the expression levels of 25 selected ribosomal protein genes, whose expression was decreased by less than −1 of log₂ FC in the Δaa_3 mutant relative to the WT strain, between the Δaa_3 and Δaa_3Δrel mutant strains. In the Δaa_3Δrel mutant, the *rel* gene encoding the major (p)ppGpp synthetase/hydrolase was null-mutated in the background of the Δaa_3 mutant. As shown in Figure 2B, the decreased expression of the ribosomal protein genes observed in the Δaa_3 mutant strain was at least partly restored in the Δaa_3Δrel mutant strain. We selected five genes that do not form an operon with each other and performed qRT-PCR to confirm the RNA sequencing results. The qRT-PCR results were consistent with those of the comparative RNA sequencing (Figure 2C). In order to confirm that the decreased expression of

---

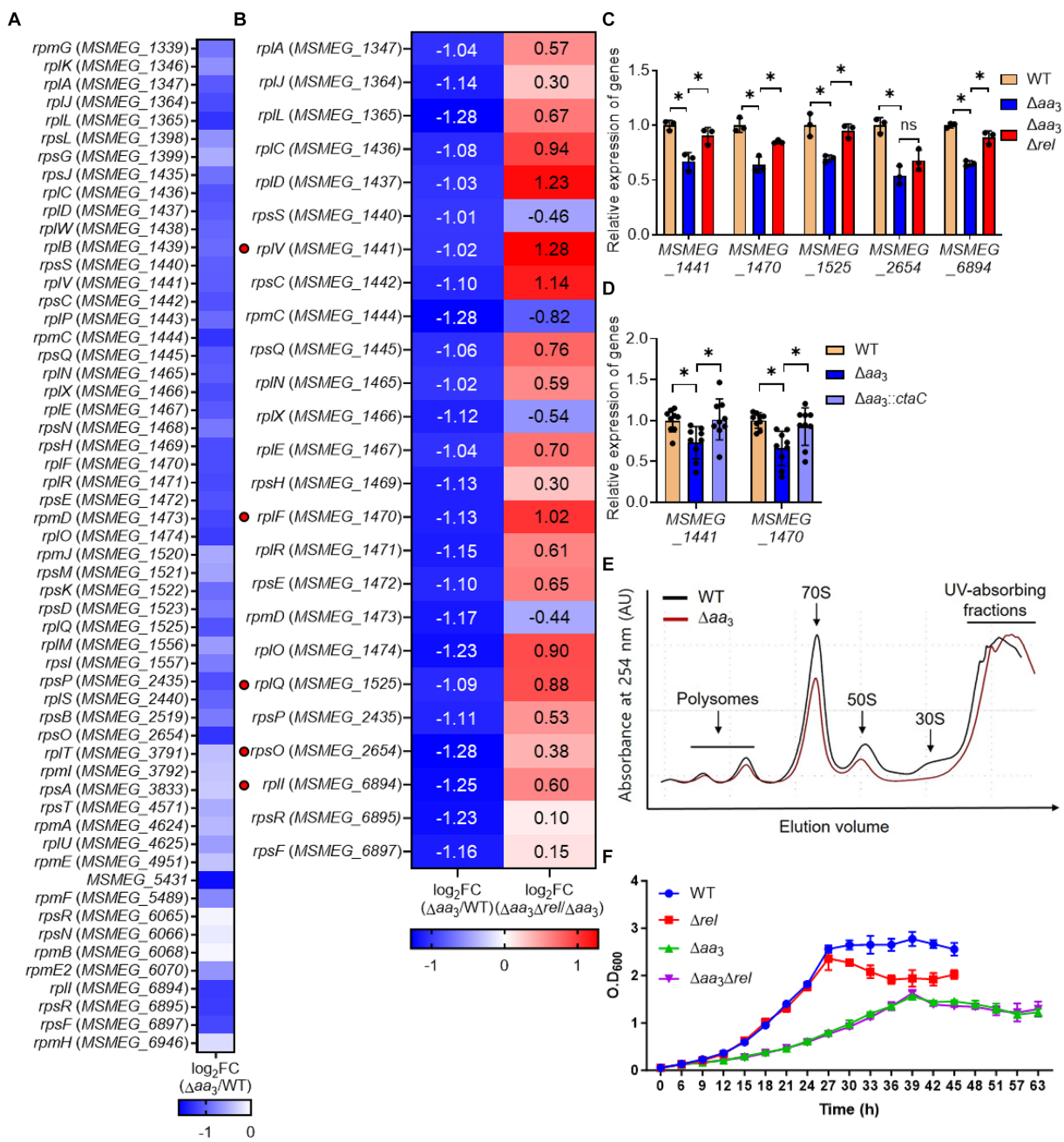[1] http://eggnog5.embl.de/

[2] https://david.ncifcrf.gov/tools.jsp

FIGURE 2

Rel-dependent decrease in the expression of the ribosomal protein genes in the Δaa₃ mutant strain relative to the WT strain and the growth curves of the WT, Δrel, Δaa₃, and Δaa₃Δrel strains. **(A)** The heatmap showing the relative expression of 56 ribosomal protein genes in the Δaa₃ mutant relative to the WT strain. The relative expression levels are expressed as log₂ FC in gene expression for the ribosomal protein genes. **(B)** The heatmap showing the log₂ FC in expression of 25 ribosomal protein genes that are significantly downregulated (log₂ FC in gene expression < −1) in the Δaa₃ mutant relative to the WT strain [log₂ FC (Δaa₃/WT)]. The heatmap also shows the log₂ FC in expression of the 25 ribosomal protein genes in the Δaa₃Δrel mutant relative to the Δaa₃ mutant [log₂ FC (Δaa₃Δrel/Δaa₃)]. The genes selected for validation by qRT-PCR are marked on the left of the heatmap with red circles. **(C)** Validation of the expression levels of the selected ribosomal protein genes (MSMEG_1441, MSMEG_1470, MSMEG_1525, MSMEG_2654, MSMEG_6894) in the WT, Δaa₃, and Δaa₃Δrel strains. The expression levels of the genes were quantitatively determined by qRT-PCR and normalized to sigA (the gene encoding the principal sigma factor) expression. The expression level of each ribosomal protein gene in the WT strain is set at 1, and the relative values are expressed for the mutant strains. **(D)** Complementation of the Δaa₃ mutant with the ctaC gene in terms of the expression of MSMEG_1441 and MSMEG_1470. For complementation of the Δaa₃ mutant, pMV306ctaC (a pMV306-derived plasmid carrying the intact ctaC gene and its own promoter) was introduced into the mutant. As control strains, the WT and mutant strains with the empty vector pMV306 were used in the experiment. The expression levels of the genes were quantitatively determined by qRT-PCR and normalized to the expression of sigA. The expression level of MSMEG_1441 or MSMEG_1470 in the WT strain with pMV306 is set at 1, and the relative values are expressed for the mutant and complemented strains. **(E)** Ribosome profiling of the WT and Δaa₃ strains. The amounts of polysomes, assembled 70S ribosomes, and ribosomal subunits were compared between the WT and Δaa₃ strains after normalizing the ribosome profiles to the absorbance of UV (254 nm)-absorbing fractions containing proteins, nucleic acids, nucleotides, and other components. **(F)** Growth curves of the WT, Δrel, Δaa₃, and Δaa₃Δrel strains in 7H9-glucose medium under aerobic conditions. All values are the means of the results from three biological replicates for panels **(A,C,F)** and nine biological replicates for panel **(D)**. The comparative RNA sequencing results between the Δaa₃ and Δaa₃Δrel strains shown in panel **(B)** were obtained from two biological replicates as described in section Materials and Methods. The error bars indicate the standard deviations. *p < 0.05. AU, arbitrary unit.

ribosomal protein genes in the Δaa_3 mutant strain is due to the deletion of *ctaC,* the Δaa_3 mutant strain was complemented with the intact *ctaC* gene using the *ctaC*-expressing plasmid pMV306ctaC. As shown in Figure 2D, the introduction of pMV306ctaC into the Δaa_3 mutant led to the restoration of the expression of *MSMEG_1441* and *MSMEG_1470* to the WT level. This indicates that the decreased expression of the ribosomal protein genes in the Δaa_3 mutant relative to the WT strain is attributed to the inactivation of the aa_3 oxidase. Ribosome profiling analysis showed that the amounts of polysomes, assembled 70S ribosomes, and ribosomal subunits were decreased in the Δaa_3 mutant, compared to the WT strain (Figure 2E). Taken together, RNA sequencing, qRT-PCR, and ribosome profiling results suggest that the expression of ribosomal protein genes and the biogenesis of ribosomes are decreased in the Δaa_3 mutant compared to the WT strain, and that this decrease in the Δaa_3 mutant strain occurs, at least in part, in a Rel-dependent way.

As judged by the growth curves of the WT and Δrel strains, the inactivation of Rel in the WT strain did not affect its aerobic growth in 7H9-glucose medium until the stationary phase (Figure 2F). However, the optical density of the Δrel mutant declined during the early stationary phase, while that of the WT strain was maintained, indicating that the absence of Rel and the resulting lack of SR induction are likely detrimental to the WT strain of *M. smegmatis* during the stationary phase. This observation is consistent with the previous report (Dahl et al., 2005). In contrast, the growth of the $\Delta aa_3\Delta rel$ strain was not different from that of Δaa_3 strain throughout all growth phases, indicating that the presence of Rel is neither beneficial nor detrimental to the growth of *M. smegmatis* under conditions that inhibit the respiratory ETC (Figure 2F).

To confirm that the expression of ribosomal protein genes is reduced when the respiratory ETC is inhibited, we examined the expression of two selected ribosomal protein genes (*MSMEG_1441* and *MSMEG_1470*) in the WT strain treated with KCN, which inhibits the aa_3 cytochrome *c* oxidase, as well as in the Δbc_1 mutant strain, where the bcc_1 complex of the respiratory ETC is inactivated by deletion of the *qcrB* gene. The cytochrome bcc_1 complex comprises the

bcc_1-aa_3 branch of the ETC with the aa_3 cytochrome *c* oxidase (Megehee et al., 2006). As a positive control gene that is induced under respiration-inhibitory conditions, we included the *cydA* gene, which encodes the catalytic subunit of the *bd* quinol oxidase, in the experiment. As shown in Figure 3A, the expression of *cydA* was significantly increased under the KCN-treated WT strain relative to the untreated control WT strain. In contrast, the expression of the ribosomal protein genes was reduced in the KCN-treated WT strain compared to the untreated WT strain. Similarly, the expression levels of the ribosomal protein genes in the Δbc_1 mutant strain was decreased to approximately 50% of those in the WT strain, while the expression of *cydA* was significantly increased in the Δbc_1 mutant strain relative to the WT strain (Figure 3B). We further examined whether the expression of the ribosomal protein genes is decreased in the WT strain when exposed to hypoxic conditions that inhibit the respiratory ETC. As depicted in Figure 3C, the expression levels of the ribosomal protein genes were decreased by more than 80% under hypoxic conditions relative to aerobic conditions, whereas the expression level of *cydA* was greatly increased under hypoxic conditions compared to aerobic conditions. By compiling several deposited transcriptomic datasets obtained from *M. smegmatis* exposed to conditions likely to inhibit the respiratory ETC such as hypoxia, bedaquiline (an inhibitor of ATP synthase) treatment, and starvation (PBS-Tween 80) due to a lack of the final electron acceptor O_2, the coupling of the ETC and ATP synthase, and a lack of electron donors, respectively, we observed that the expression of the genes encoding the ribosomal proteins and RNA polymerase was decreased under the tested conditions, similar to the Δaa_3 mutant (Figure 4). The decrease effect was more noticeable under the well-known SR-inducing starvation condition relative to the Δaa_3 mutant, indicating that the extent of SR induction in the Δaa_3 mutant is not as strong as that under starvation conditions. Collectively, these results confirm a decrease in the expression of ribosomal protein genes under conditions that inhibit the respiratory ETC.

The observed decrease in the expression of the ribosomal protein genes in the Δaa_3 mutant strain in a Rel-dependent
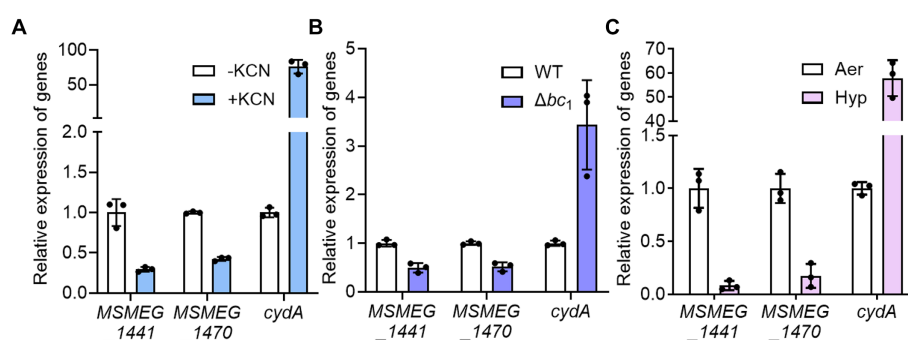

FIGURE 3
Effects of inhibiting the respiratory ETC on the expression of *MSMEG_1441* and *MSMEG_1470*. **(A)** The expression levels of *cydA* and the two ribosomal protein genes in the WT strain with or without KCN treatment. The WT strains were aerobically grown to an OD_{600} of 0.45−0.5 and further grown for 2 h either after treatment with 50 μM KCN (+KCN) or without KCN treatment as a control (−KCN). **(B)** The expression levels of *cydA* and the two ribosomal protein genes in the WT and Δbc_1 mutant strains grown aerobically to an OD_{600} of 0.45−0.5. **(C)** The expression levels of *cydA* and the two ribosomal protein genes in the WT grown under aerobic (Aer) or hypoxic (Hyp) conditions. The expression levels of *cydA*, *MSMEG_1441,* and *MSMEG_1470* were determined by qRT-PCR and normalized to that of *sigA*. The expression level of each gene in the control WT strains is set at 1, and the relative values are expressed for the KCN-treated, hypoxically grown WT, and the Δbc_1 mutant. All values provided are the averages of the results from three biological replicates. The error bars indicate the standard deviations.
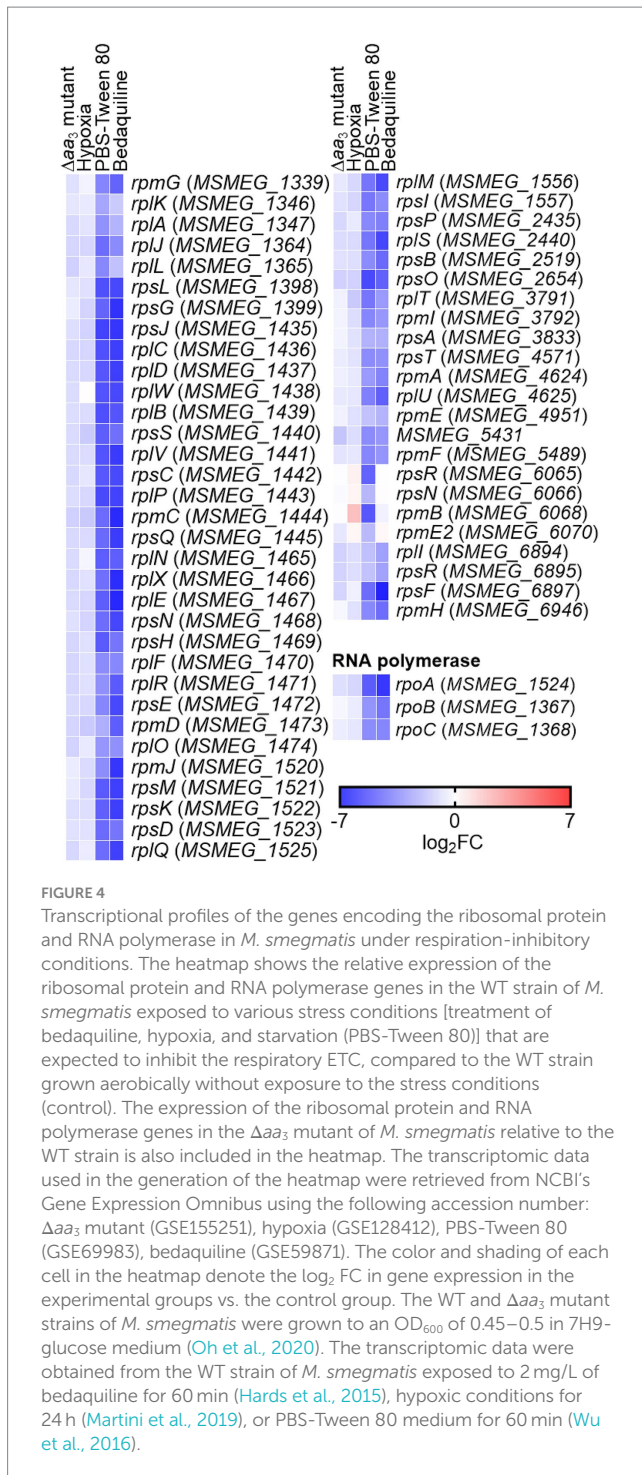
FIGURE 4

Transcriptional profiles of the genes encoding the ribosomal protein and RNA polymerase in *M. smegmatis* under respiration-inhibitory conditions. The heatmap shows the relative expression of the ribosomal protein and RNA polymerase genes in the WT strain of *M. smegmatis* exposed to various stress conditions [treatment of bedaquiline, hypoxia, and starvation (PBS-Tween 80)] that are expected to inhibit the respiratory ETC, compared to the WT strain grown aerobically without exposure to the stress conditions (control). The expression of the ribosomal protein and RNA polymerase genes in the Δaa₃ mutant of *M. smegmatis* relative to the WT strain is also included in the heatmap. The transcriptomic data used in the generation of the heatmap were retrieved from NCBI's Gene Expression Omnibus using the following accession number: Δaa₃ mutant (GSE155251), hypoxia (GSE128412), PBS-Tween 80 (GSE69983), bedaquiline (GSE59871). The color and shading of each cell in the heatmap denote the log₂ FC in gene expression in the experimental groups vs. the control group. The WT and Δaa₃ mutant strains of *M. smegmatis* were grown to an OD₆₀₀ of 0.45–0.5 in 7H9-glucose medium (Oh et al., 2020). The transcriptomic data were obtained from the WT strain of *M. smegmatis* exposed to 2 mg/L of bedaquiline for 60 min (Hards et al., 2015), hypoxic conditions for 24 h (Martini et al., 2019), or PBS-Tween 80 medium for 60 min (Wu et al., 2016).

FIGURE 5

Verification of SR induction in the Δaa₃ mutant of *M. smegmatis* by determining the expression levels of the *eis* and *wag31* genes. **(A)** Expression of *eis* in the WT strain grown under glucose-replete (0.2%) and glucose-limiting (0.01%) conditions. **(B)** Expression of *eis* in the WT and Δaa₃ mutant strains. **(C)** Expression of *wag31* in the WT strain grown under glucose-replete and glucose-limiting conditions. **(D)** Expression of *wag31* in the WT and Δaa₃ mutant strains. The WT and Δaa₃ mutant strains containing the *eis*::*lacZ* and *wag31*::*lacZ* translational fusion plasmids, pNCIIeis and pNCIIwag31, were used to measure the expression levels of *eis* and *wag31*, respectively. The WT and Δaa₃ mutant strains were grown aerobically to an OD₆₀₀ of 0.45 to 0.5 in 7H9-glucose medium. Cell-free crude extracts were used to measure β-galactosidase activity. All values provided were determined from three biological replicates. The error bars indicate the standard deviations. *p<0.05.

modulating autophagy, inflammatory responses, and cell death (Dahl et al., 2005; Shin et al., 2010). The *wag31* gene encodes the DivIVA protein that regulates cell shape and cell division in Gram-positive bacteria (Cha and Stewart, 1997; Flardh, 2003). The expression of the *eis* and *wag31* genes of *M. tuberculosis* has been previously demonstrated to be decreased and increased, respectively, in *M. smegmatis* under SR-inducing conditions in a Rel-dependent manner, when the genes with their own promoters were introduced into *M. smegmatis* (Dahl et al., 2005; Dahl and Lau Bonilla, 2011). First, we reaffirmed whether the expression of the *eis* and *wag31* genes is altered in *M. smegmatis* under a nutrient starvation condition that induces the SR. The WT strains of *M. smegmatis* with the *eis*::*lacZ* or *wag31*::*lacZ* translational fusion plasmid (pNCIIeis or pNCIIwag31) were assessed for the expression levels of the two reporter genes after growth in 7H9 medium supplemented with 0.01% glucose for nutrient starvation and 0.2% glucose for the control (Figures 5A,C). As reported

manner led us to assume that SR is induced under respiration-inhibitory conditions. Because it was difficult for us to quantitatively measure changes in intracellular (p)ppGpp levels in the Δaa₃ mutant where a strong SR does not occur, we instead examined whether SR is induced in the Δaa₃ mutant strain by comparatively determining the expression of the *eis* (*Rv2416c*) and *wag31* (*Rv2145c*) genes of *M. tuberculosis* in the WT and Δaa₃ mutant strains of *M. smegmatis*. The *eis* gene encodes the enhanced intracellular survival protein that was suggested to be involved in suppressing host innate immune defenses by
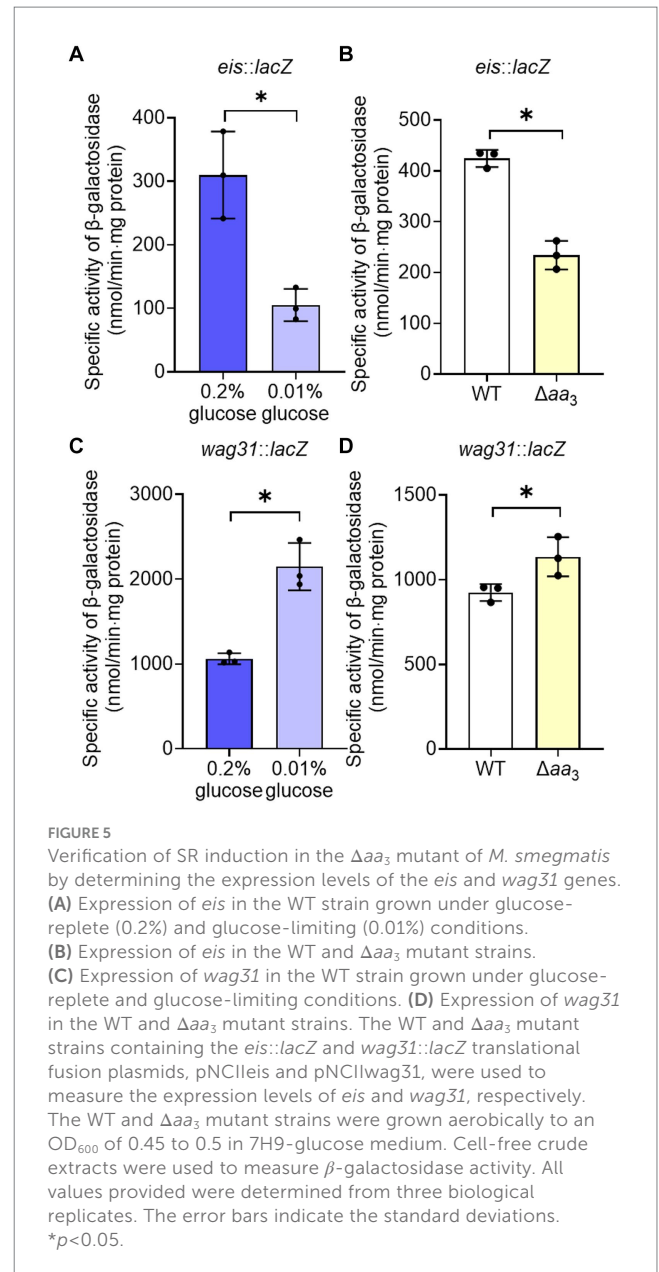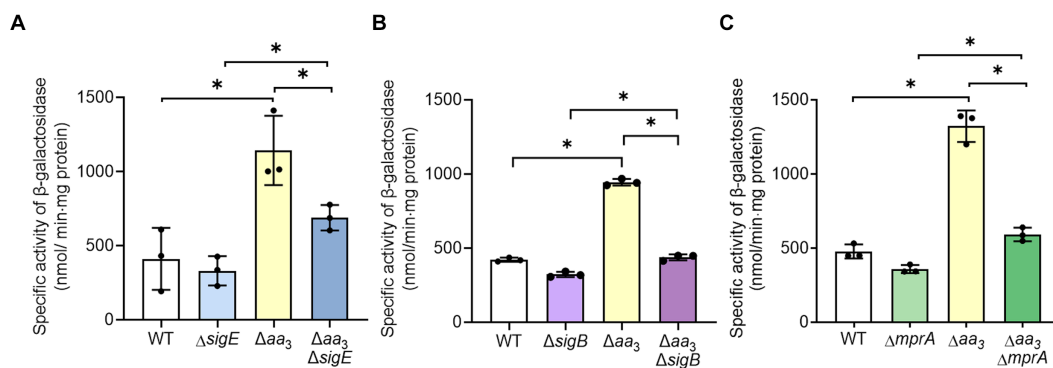
FIGURE 6
Involvement of the MprBA-SigE-SigB regulatory pathway in the upregulation of the *rel* gene in the Δ*aa₃* mutant of *M. smegmatis*. **(A)** Expression of *rel* in the WT, Δ*sigE*, Δ*aa₃*, and Δ*aa₃*Δ*sigE* strains. **(B)** Expression of *rel* in the WT, Δ*sigB*, Δ*aa₃*, and Δ*aa₃*Δ*sigB* strains. **(C)** Expression of *rel* in the WT, Δ*mprA*, Δ*aa₃*, and Δ*aa₃*Δ*mprA* strains. The expression level of the *rel* gene in the WT and mutant strains was measured using the *rel::lacZ* translational fusion plasmid pNCIIrel. The WT and mutant strains containing pNCIIrel were grown aerobically to an OD_{600} of 0.45 to 0.5 in 7H9-glucose medium. Cell-free crude extracts were used to measure *β*-galactosidase activity. All values provided were determined from three biological replicates. The error bars indicate the standard deviations. *$p < 0.05$.
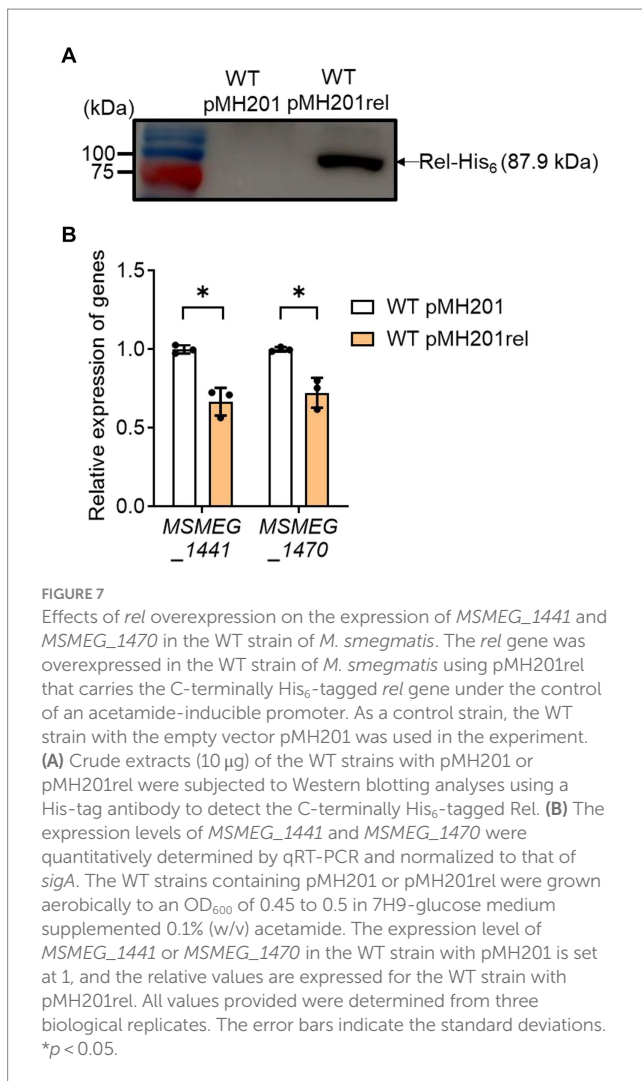
previously (Dahl et al., 2005; Dahl and Lau Bonilla, 2011), the expression level of *eis* was decreased, while that of *wag31* was increased under glucose starvation (0.01%) relative to those in the WT strain supplemented with 0.2% glucose. As shown in Figure 5B, the expression level of *eis* was decreased in the Δ*aa₃* mutant strain relative to that in the WT strain. In contrast, the expression level of *wag31* was slightly increased in the Δ*aa₃* mutant strain relative to that in the WT strain (Figure 5D). These results support our assumption that SR is to some extent induced in the Δ*aa₃* mutant.

Increased expression of *rel* and induction of SR through the MprBA-SigE-SigB regulatory pathway under conditions that inhibit the respiratory ETC

Given the finding that SR is induced in the Δ*aa₃* mutant, we sought to investigate how SR is induced in the Δ*aa₃* mutant. One possibility is that the expression of a gene encoding the enzyme that produces (p)ppGpp is increased in the Δ*aa₃* mutant. There are two (p)ppGpp synthetases, Rel and RelZ, in *M. smegmatis* (Murdeshwar and Chatterji, 2012). According to our RNA sequencing results, the reads per kilobase per million mapped reads (RPKM) value of *rel* was 5.1-fold higher than that of *relZ* in the WT strain of *M. smegmatis* grown aerobically, indicating that Rel is the predominantly expressed (p)ppGpp synthetase in *M. smegmatis* (data not shown). Furthermore, our RNA sequencing results showed that the expression of *rel* was increased 1.3-fold in the Δ*aa₃* mutant relative to the WT strain, while the expression of *relZ* was not different between the WT and Δ*aa₃* mutant strains (data not shown). To verify whether the expression of *rel* is increased in the Δ*aa₃* mutant compared to the WT strain, we assessed the expression level of *rel* in the WT and Δ*aa₃* mutant strains using the *rel::lacZ* translational fusion pNCIIrel. As shown in Figure 6, the *β*-galactosidase assay showed that the expression of *rel* was more than two-fold higher in the Δ*aa₃* mutant relative to the WT strain when both strains were grown aerobically. The expression of *rel*

is known to be regulated by the alternative sigma factor SigE. SigE was suggested to be one of the central nodes of the regulatory network involved in SR in mycobacteria (Sureka et al., 2007). Furthermore, it was demonstrated that transcription of *sigB*, which encodes another alternative sigma factor, strictly depends on SigE, and that the SigE-SigB regulatory pathway is activated in the Δ*aa₃* mutant of *M. smegmatis* (Oh et al., 2022). To examine whether the increased expression of *rel* in the Δ*aa₃* mutant is attributed to SigE and SigB, the expression of the *rel* gene was comparatively determined in the WT, Δ*sigE*, Δ*sigB*, Δ*aa₃*, Δ*aa₃*Δ*sigE*, and Δ*aa₃*Δ*sigB* strains of *M. smegmatis* carrying pNCIIrel (Figures 6A,B). In the Δ*aa₃*Δ*sigE* mutant, the expression level of *rel* was reduced to an intermediate level between those in the WT and Δ*aa₃* mutant strains (Figure 6A). The expression level of *rel* in the Δ*aa₃*Δ*sigB* mutant was shown to be only slightly increased compared to that observed for the Δ*sigB* mutant (Figure 6B). Considering the hierarchical order of SigE and SigB in the SigE-SigB signaling pathway and the stricter dependence on SigB than SigE for the upregulation of *rel* expression in the Δ*aa₃* mutant, these results suggest that SigB, rather than SigE, is directly involved in the upregulation of *rel* in the Δ*aa₃* mutant. Since the MprA response regulator of the MprBA TCS is known to positively regulate the expression of *sigE* in mycobacteria (He et al., 2006), we assessed whether MprA is involved in the upregulation of *rel* expression in the Δ*aa₃* mutant. For this purpose, the expression level of *rel* was comparatively determined in the WT, Δ*mprA*, Δ*aa₃*, and Δ*aa₃*Δ*mprA* strains of *M. smegmatis* carrying pNCIIrel (Figure 6C). In the Δ*aa₃*Δ*mprA* mutant, the increased expression of *rel* observed for the Δ*aa₃* mutant relative to the WT strain was almost abolished, which indicates that the MprBA TCS is required for the upregulation of *rel* expression caused by the inactivation of the *aa₃* oxidase. Taken together, the results presented in Figure 6 suggest that respiration inhibition such as the inactivation of the *aa₃* oxidase brings about an increase in *rel* expression through the MprBA-SigE-SigB signaling pathway.

Next, we examined whether an increase in *rel* expression results in a decrease in the expression of ribosomal protein genes in the WT strain of *M. smegmatis* (Figure 7). The *rel* gene was

FIGURE 7
Effects of *rel* overexpression on the expression of *MSMEG_1441* and *MSMEG_1470* in the WT strain of *M. smegmatis*. The *rel* gene was overexpressed in the WT strain of *M. smegmatis* using pMH201rel that carries the C-terminally His$_6$-tagged *rel* gene under the control of an acetamide-inducible promoter. As a control strain, the WT strain with the empty vector pMH201 was used in the experiment. **(A)** Crude extracts (10 μg) of the WT strains with pMH201 or pMH201rel were subjected to Western blotting analyses using a His-tag antibody to detect the C-terminally His$_6$-tagged Rel. **(B)** The expression levels of *MSMEG_1441* and *MSMEG_1470* were quantitatively determined by qRT-PCR and normalized to that of *sigA*. The WT strains containing pMH201 or pMH201rel were grown aerobically to an OD$_{600}$ of 0.45 to 0.5 in 7H9-glucose medium supplemented 0.1% (w/v) acetamide. The expression level of *MSMEG_1441* or *MSMEG_1470* in the WT strain with pMH201 is set at 1, and the relative values are expressed for the WT strain with pMH201rel. All values provided were determined from three biological replicates. The error bars indicate the standard deviations. *$p < 0.05$.

FIGURE 8
RNA sequencing results showing the involvement of the MprBA TCS in the downregulation of the ribosomal protein genes in the Δ*aa$_3$* mutant of *M. smegmatis*. The heatmap shows the log$_2$ FC in expression of 25 ribosomal protein genes that are significantly downregulated (log$_2$ FC in gene expression < −1) in the Δ*aa$_3$* mutant relative to the WT strain [log$_2$ FC (Δ*aa$_3$*/WT)], as well as the log$_2$ FC in expression of the 25 ribosomal protein genes in the Δ*aa$_3$*Δ*mprA* mutant relative to the Δ*aa$_3$* mutant [log$_2$ FC (Δ*aa$_3$*Δ*mprA*/Δ*aa$_3$*)].

overexpressed in the presence of acetamide using pMH201rel, in which the C-terminally His$_6$-tagged *rel* gene is expressed by an acetamide-inducible promoter. Western blotting analysis using a His-tag antibody showed that the His$_6$-tagged Rel protein was expressed in the WT strain carrying pMH201rel, while no band was observed at the corresponding position in case of the WT strain with the empty vector pMH201 (Figure 7A). The expression levels of *MSMEG_1441* and *MSMEG_1470* were reduced in the WT strain with pMH201rel by about 30% compared to those in the WT strain with pMH201 (Figure 7B), suggesting the possibility that the induction of SR in the Δ*aa$_3$* mutant is at least partly attributable to the increased expression of *rel* in the mutant. Given the positive correlation of the extent of *rel* expression with SR induction, as well as the abolishment of an increase in *rel* expression in the Δ*aa$_3$* mutant by the null mutation of *mprA*, we assumed that the SR induced in the Δ*aa$_3$* mutant could be abolished in the Δ*aa$_3$*Δ*mprA* mutant. To examine this assumption, we compared the expression levels of 25 selected ribosomal protein genes, whose expression was decreased by less than −1 of log$_2$ FC in the Δ*aa$_3$* mutant relative to the WT strain, between the Δ*aa$_3$* and Δ*aa$_3$*Δ*mprA* mutant strains. As shown in Figure 8, the decreased expression of the ribosomal protein genes
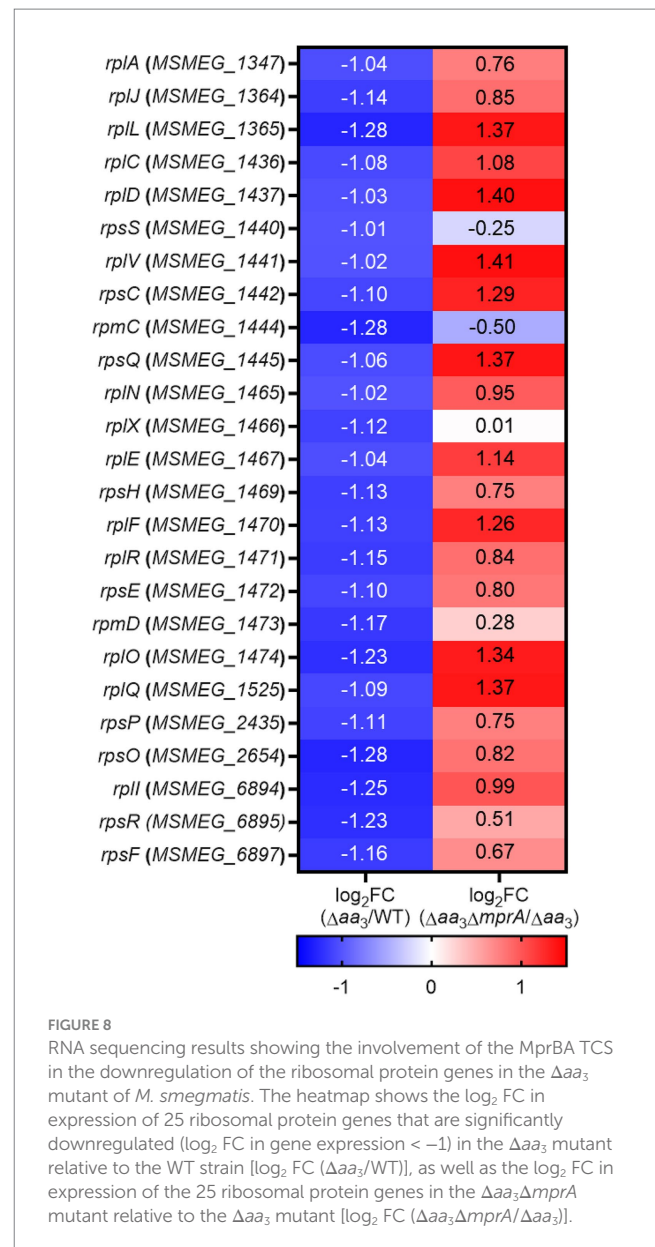
observed in the Δ*aa$_3$* mutant strain was mostly restored in the Δ*aa$_3$*Δ*mprA* mutant strain.
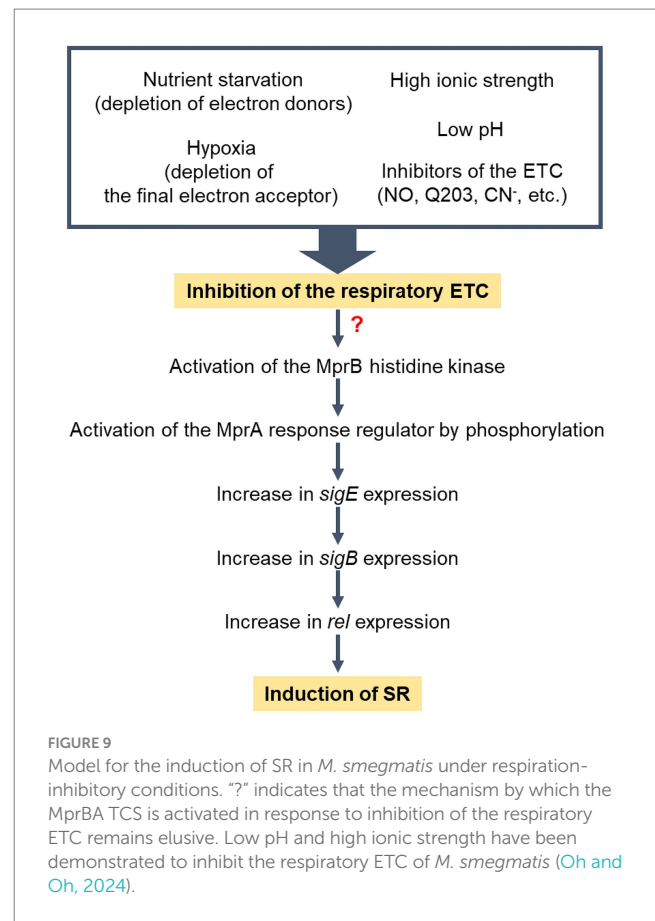
Discussion

When the SR is induced, it is known to affect many aspects of cellular metabolism, including central dogma processes such as transcription and translation. These alterations elicit physiological changes, such as a general slowdown of protein synthesis and growth (Legault et al., 1972; Corrigan et al., 2016), which aids bacterial adaptation and survival under stress conditions. The regulation of gene expression by SR in mycobacteria exhibits similarities to the conventional SR: the expression of genes related with ribosome biogenesis, as well as those encoding RNA polymerase, is downregulated in a

Rel-dependent way under SR-inducing conditions (Stallings et al., 2009). In mycobacteria, SR has been demonstrated to be induced when they were exposed to nutrient starvation, oxidative stress, and hypoxic conditions (Avarbock et al., 2000; Primm et al., 2000; Betts et al., 2002; Stallings et al., 2009).

In this study, we presented several lines of evidence that support the induction of SR in *M. smegmatis* under conditions that inhibit the respiratory ETC. Our RNA sequencing results showed that the expression of most ribosomal protein genes and RNA polymerase genes was decreased in the aerobically grown Δaa_3 mutant strain compared to the WT strain grown under the same conditions. As in the Δaa_3 mutant, the expression levels of two representative ribosomal protein genes, *MSMEG_1441* and *MSMEG_1470*, were shown to decrease under conditions that inhibit the respiratory ETC, such as treatment of KCN, inactivation of the cytochrome bcc_1 complex, and hypoxic conditions. Furthermore, the previous transcriptomic datasets have shown that the expression of the ribosomal protein genes is reduced in *M. smegmatis* treated with bedaquiline, as well as in *M. smegmatis* exposed to hypoxic conditions. These results support our assumption that inhibition of the respiratory ETC leads to SR induction in *M. smegmatis*. Furthermore, changes in the expression of the known SR-responsive genes *eis* and *wag31* in the Δaa_3 mutant corroborated our assumption that SR is indeed induced in the Δaa_3 mutant. The reduced expression of ribosomal protein genes in the Δaa_3 mutant was recovered by a null mutation of *rel*, which indicates Rel-dependent induction of SR in the Δaa_3 mutant. Our findings that the expression of *rel* is increased in the Δaa_3 mutant and that overexpression of *rel* leads to the decreased expression of two ribosomal protein genes, *MSMEG_1441* and *MSMEG_1470*, suggest that the elevated expression of *rel* under respiration-inhibitory conditions contributes to SR induction in *M. smegmatis*.

Previously it has been reported that the expression of *rel* in *M. smegmatis* is regulated via the MprBA-SigE regulatory pathway, in which the MprBA TCS positively regulates the expression of *sigE* (He et al., 2006; Sureka et al., 2007). SigE was suggested to be an alternative sigma factor that participates in transcription of *rel* (Sureka et al., 2007). Our recent RNA sequencing analysis revealed that the expression of the SigE and SigB regulons is increased in the Δaa_3 mutant strain of *M. smegmatis* compared to that in the WT strain, which is attributable to both the increased expression of *sigE* in the mutant and the SigE-dependent transcription of *sigB* (Oh et al., 2022). Together with the previous finding that the expression of *sigE* is significantly increased in the $\Delta sigB$ mutant relative to the WT strain (Oh et al., 2022), the results of our comparative determination of *rel* expression in the WT, $\Delta sigB$, $\Delta sigE$, Δaa_3, $\Delta aa_3\Delta sigB$, and $\Delta aa_3\Delta sigE$ strains of *M. smegmatis* suggest that SigB, rather than SigE, is directly involved in the increased expression of *rel* in the Δaa_3 mutant (Figure 6). Furthermore, the expression of ribosomal protein genes was found to be restored in the $\Delta aa_3\Delta mprA$ mutant relative to the Δaa_3 mutant. Additionally, the increased expression of *rel* in the Δaa_3 mutant was found to require the MprBA TCS. Based on these results, we propose that the induction of SR by an increase in *rel* expression in the Δaa_3 mutant is mediated through the MprBA-SigE-SigB regulatory pathway (Figure 9). However, the

FIGURE 9
Model for the induction of SR in *M. smegmatis* under respiration-inhibitory conditions. "?" indicates that the mechanism by which the MprBA TCS is activated in response to inhibition of the respiratory ETC remains elusive. Low pH and high ionic strength have been demonstrated to inhibit the respiratory ETC of *M. smegmatis* (Oh and Oh, 2024).

mechanism by which the MprBA TCS is activated in response to inhibition of the respiratory ETC remains currently elusive. Further studies are required to answer this question. Since polyphosphate itself can serve as a phosphate donor for MprB, certain regulatory systems involved in regulating intracellular levels of polyphosphate could interconnect with the MprBA-SigE-SigB-Rel pathway to form a regulatory network for SR induction. Supporting this assumption, the depletion of inorganic phosphate has been demonstrated to lead to increased expression of *sigE* and *rel* in *M. tuberculosis* through the SenX3-RegX3 TCS that is responsible for inorganic phosphate sensing and is involved in regulating the expression of the *ppk1* gene encoding polyphosphate kinase (Rifat et al., 2009).

In conclusion, we propose that SR is induced in *M. smegmatis* under respiration-inhibitory conditions. This event appears to be primarily mediated by the MprBA-SigE-SigB-Rel pathway. Since respiration-inhibitory conditions encompass a wide range of factors that hinder the functionality of the respiratory ETC, various extracellular and intracellular conditions that can disrupt the functionality of the respiratory ETC are expected to be integrated and induce SR. They include conditions in which electron donors or terminal electron acceptors of the ETC are deficient such as nutrient starvation and hypoxia, conditions in which respiratory ETC components are inhibited such as ETC inhibitor treatment and ETC mutants, and conditions in which the proton motive force and membrane potential are affected so that the ETC is inhibited such as low pH, high ionic strength, and inhibition of the F_o/F_1 ATP synthase.

Data availability statement

The datasets presented in this study can be found in online repositories. The names of the repository/repositories and accession number(s) can be found at: https://www.ncbi.nlm.nih.gov/geo/, GSE155251, GSE267048, GSE128412, GSE69983, and GSE59871.

Author contributions

N-KK: Data curation, Formal analysis, Investigation, Writing – original draft. J-EB: Investigation, Writing – original draft. Y-JL: Investigation, Writing – original draft. YO: Data curation, Formal analysis, Investigation, Writing – original draft. J-IO: Conceptualization, Funding acquisition, Supervision, Writing – review & editing.

Funding

Conflict of interest

The authors declare that the research was conducted in the absence of any commercial or financial relationships that could be construed as a potential conflict of interest.

Publisher's note

All claims expressed in this article are solely those of the authors and do not necessarily represent those of their affiliated organizations, or those of the publisher, the editors and the reviewers. Any product that may be evaluated in this article, or claim that may be made by its manufacturer, is not guaranteed or endorsed by the publisher.

Supplementary material

The Supplementary material for this article can be found online at: https://www.frontiersin.org/articles/10.3389/fmicb.2024.1448277/full#supplementary-material

References

Avarbock, D., Avarbock, A., and Rubin, H. (2000). Differential regulation of opposing Rel_Mtb activities by the aminoacylation state of a tRNA.Ribosome.mRNA.Rel_Mtb complex. *Biochemistry* 39, 11640–11648. doi: 10.1021/bi001256k

Avarbock, A., Avarbock, D., Teh, J. S., Buckstein, M., Wang, Z. M., and Rubin, H. (2005). Functional regulation of the opposing (p)ppGpp synthetase/hydrolase activities of Rel_Mtb from *Mycobacterium tuberculosis*. *Biochemistry* 44, 9913–9923. doi: 10.1021/bi0505316

Avarbock, D., Salem, J., Li, L. S., Wang, Z. M., and Rubin, H. (1999). Cloning and characterization of a bifunctional RelA/SpoT homologue from *Mycobacterium tuberculosis*. *Gene* 233, 261–269. doi: 10.1016/s0378-1119(99)00114-6

Bag, S., Das, B., Dasgupta, S., and Bhadra, R. K. (2014). Mutational analysis of the (p)ppGpp synthetase activity of the Rel enzyme of *Mycobacterium tuberculosis*. *Arch. Microbiol.* 196, 575–588. doi: 10.1007/s00203-014-0996-9

Baker, J. J., and Abramovitch, R. B. (2018). Genetic and metabolic regulation of *Mycobacterium tuberculosis* acid growth arrest. *Sci. Rep.* 8:4168. doi: 10.1038/s41598-018-22343-4

Bange, G., Brodersen, D. E., Liuzzi, A., and Steinchen, W. (2021). Two P or not two P: understanding regulation by the bacterial second messengers (p)ppGpp. *Ann. Rev. Microbiol.* 75, 383–406. doi: 10.1146/annurev-micro-042621-122343

Beites, T., O'Brien, K., Tiwari, D., Engelhart, C. A., Walters, S., Andrews, J., et al. (2019). Plasticity of the *Mycobacterium tuberculosis* respiratory chain and its impact on tuberculosis drug development. *Nat. Commun.* 10, 4970–4912. doi: 10.1038/s41467-019-12956-2

Belevich, I., Borisov, V. B., Bloch, D. A., Konstantinov, A. A., and Verkhovsky, M. I. (2007). Cytochrome *bd* from *Azotobacter vinelandii*: evidence for high-affinity oxygen binding. *Biochemistry* 46, 11177–11184. doi: 10.1021/bi700862u

Betts, J. C., Lukey, P. T., Robb, L. C., McAdam, R. A., and Duncan, K. (2002). Evaluation of a nutrient starvation model of *Mycobacterium tuberculosis* persistence by gene and protein expression profiling. *Mol. Microbiol.* 43, 717–731. doi: 10.1046/j.1365-2958.2002.02779.x

Bretl, D. J., Demetriadou, C., and Zahrt, T. C. (2011). Adaptation to environmental stimuli within the host: two-component signal transduction systems of *Mycobacterium tuberculosis*. *Microbiol. Mol. Biol. Rev.* 75, 566–582. doi: 10.1128/MMBR.05004-11

Cha, J. H., and Stewart, G. C. (1997). The divIVA minicell locus of *Bacillus subtilis*. *J. Bacteriol.* 179, 1671–1683. doi: 10.1128/jb.179.5.1671-1683.1997

Corrigan, R. M., Bellows, L. E., Wood, A., and Grundling, A. (2016). ppGpp negatively impacts ribosome assembly affecting growth and antimicrobial tolerance in gram-positive bacteria. *Proc. Natl. Acad. Sci. USA* 113, E1710–E1719. doi: 10.1073/pnas.1522179113

Dahl, J. L., Arora, K., Boshoff, H. I., Whiteford, D. C., Pacheco, S. A., Walsh, O. J., et al. (2005). The *relA* homolog of *Mycobacterium smegmatis* affects cell appearance, viability, and gene expression. *J. Bacteriol.* 187, 2439–2447. doi: 10.1128/jb.187.7.2439-2447.2005

Dahl, J. L., Kraus, C. N., Boshoff, H. I. M., Doan, B., Foley, K., Avarbock, D., et al. (2003). The role of Rel_Mtb-mediated adaptation to stationary phase in long-term persistence of *Mycobacterium tuberculosis* in mice. *Proc. Natl. Acad. Sci. USA* 100, 10026–10031. doi: 10.1073/pnas.1631248100

Dahl, J. L., and Lau Bonilla, D. (2011). The *wag31* gene of *Mycobacterium tuberculosis* is positively regulated by the stringent response. *FEMS Microbiol. Lett.* 319, 153–159. doi: 10.1111/j.1574-6968.2011.02278.x

Dutta, N. K., Klinkenberg, L. G., Vazquez, M. J., Segura-Carro, D., Colmenarejo, G., Ramon, F., et al. (2019). Inhibiting the stringent response blocks *Mycobacterium tuberculosis* entry into quiescence and reduces persistence. *Sci. Adv.* 5:eaav2104. doi: 10.1126/sciadv.aav2104

Flardh, K. (2003). Essential role of DivIVA in polar growth and morphogenesis in *Streptomyces coelicolor* A3(2). *Mol. Microbiol.* 49, 1523–1536. doi: 10.1046/j.1365-2958.2003.03660.x

Green, M. R., and Sambrook, J. (2012). Molecular cloning: a laboratory manual. *4th* Edn. New York, NY: Cold Spring Harbor Laboratory Press.

Gupta, K. R., Arora, G., Mattoo, A., and Sajid, A. (2021). Stringent response in mycobacteria: from biology to therapeutic potential. *Pathogens* 10:1417. doi: 10.3390/pathogens10111417

Gupta, K. R., Baloni, P., Indi, S. S., and Chatterji, D. (2016). Regulation of growth, cell shape, cell division, and gene expression by second messengers (p)ppGpp and cyclic di-GMP in *Mycobacterium smegmatis*. *J. Bacteriol.* 198, 1414–1422. doi: 10.1128/jb.00126-16

Hards, K., Robson, J. R., Berney, M., Shaw, L., Bald, D., Koul, A., et al. (2015). Data from: Bactericidal mode of action of bedaquiline. Gene Expression Omnibus. Available at: https://www.ncbi.nlm.nih.gov/geo/query/acc.cgi?acc=GSE59871

He, H., Hovey, R., Kane, J., Singh, V., and Zahrt, T. C. (2006). MprAB is a stress-responsive two-component system that directly regulates expression of sigma factors SigB and SigE in *Mycobacterium tuberculosis*. *J. Bacteriol.* 188, 2134–2143. doi: 10.1128/JB.188.6.2134-2143.2006

Huang da, W., Sherman, B. T., and Lempicki, R. A. (2009). Systematic and integrative analysis of large gene lists using DAVID bioinformatics resources. *Nat. Protoc.* 4, 44–57. doi: 10.1038/nprot.2008.211

Huerta-Cepas, J., Szklarczyk, D., Heller, D., Hernandez-Plaza, A., Forslund, S. K., Cook, H., et al. (2019). eggNOG 5.0: a hierarchical, functionally and phylogenetically annotated orthology resource based on 5090 organisms and 2502 viruses. *Nucleic Acids Res.* 47, D309–D314. doi: 10.1093/nar/gky1085

Jain, V., Saleem-Batcha, R., China, A., and Chatterji, D. (2006). Molecular dissection of the mycobacterial stringent response protein Rel. *Protein Sci.* 15, 1449–1464. doi: 10.1110/ps.062117006

Jeong, J. A., Lee, H. N., Ko, I. J., and Oh, J. I. (2013). Development of new vector systems as genetic tools applicable to mycobacteria. *J. Life Science* 23, 290–298. doi: 10.5352/JLS.2013.23.2.290

Jeong, J. A., Park, S. W., Yoon, D., Kim, S., Kang, H. Y., and Oh, J. I. (2018). Roles of alanine dehydrogenase and induction of its gene in *Mycobacterium smegmatis* under respiration-inhibitory conditions. *J. Bacteriol.* 200, e00152–18. doi: 10.1128/JB.00152-18

Jessee, J. (1986). New subcloning efficiency competent cells: >1x10⁶ transformants/µg. *Focus* 8, 1146–1157.

Kana, B. D., Weinstein, E. A., Avarbock, D., Dawes, S. S., Rubin, H., and Mizrahi, V. (2001). Characterization of the *cydAB*-encoded cytochrome *bd* oxidase from *Mycobacterium smegmatis*. *J. Bacteriol.* 183, 7076–7086. doi: 10.1128/JB.183.24.7076-7086.2001

Kang, C. M., Abbott, D. W., Park, S. T., Dascher, C. C., Cantley, L. C., and Husson, R. N. (2005). The *Mycobacterium tuberculosis* serine/threonine kinases PknA and PknB: substrate identification and regulation of cell shape. *Genes Dev.* 19, 1692–1704. doi: 10.1101/gad.1311105

Kim, M. J., Park, K. J., Ko, I. J., Kim, Y. M., and Oh, J. I. (2010). Different roles of DosS and DosT in the hypoxic adaptation of mycobacteria. *J. Bacteriol.* 192, 4868–4875. doi: 10.1128/JB.00550-10

Klinkenberg, L. G., Lee, J. H., Bishai, W. R., and Karakousis, P. C. (2010). The stringent response is required for full virulence of *Mycobacterium tuberculosis* in Guinea pigs. *J. Infect. Dis.* 202, 1397–1404. doi: 10.1086/656524

Ko, E. M., and Oh, J. I. (2020). Induction of the *cydAB* operon encoding the *bd* quinol oxidase under respiration-inhibitory conditions by the major cAMP receptor protein MSMEG_6189 in *Mycobacterium smegmatis*. *Front. Microbiol.* 11:608624. doi: 10.3389/fmicb.2020.608624

Krishnan, S., and Chatterji, D. (2020). Pleiotropic effects of bacterial small alarmone synthetases: underscoring the dual-domain small alarmone synthetases in *Mycobacterium smegmatis*. *Front. Microbiol.* 11:594024. doi: 10.3389/fmicb.2020.594024

Krishnan, S., Petchiappan, A., Singh, A., Bhatt, A., and Chatterji, D. (2016). R-loop induced stress response by second (p)ppGpp synthetase in *Mycobacterium smegmatis*: functional and domain interdependence. *Mol. Microbiol.* 102, 168–182. doi: 10.1111/mmi.13453

Legault, L., Jeantet, C., and Gros, F. (1972). Inhibition of *in vitro* protein synthesis by ppGpp. *FEBS Lett.* 27, 71–75. doi: 10.1016/0014-5793(72)80412-5

Martini, M. C., Zhou, Y., Sun, H., and Shell, S. S. (2019). Data from: Defining the transcriptional and post-transcriptional landscapes of *Mycobacterium smegmatis* in aerobic growth and hypoxia. Gene Expression Omnibus. Available at: https://www.ncbi.nlm.nih.gov/geo/query/acc.cgi?acc=GSE128412

Matsoso, L. G., Kana, B. D., Crellin, P. K., Lea-Smith, D. J., Pelosi, A., Powell, D., et al. (2005). Function of the cytochrome bc_1-aa_3 branch of the respiratory network in mycobacteria and network adaptation occurring in response to its disruption. *J. Bacteriol.* 187, 6300–6308. doi: 10.1128/JB.187.18.6300-6308.2005

Megehee, J. A., Hosler, J. P., and Lundrigan, M. D. (2006). Evidence for a cytochrome bcc-aa_3 interaction in the respiratory chain of *Mycobacterium smegmatis*. *Microbiology* 152, 823–829. doi: 10.1099/mic.0.28723-0

Mouncey, N. J., and Kaplan, S. (1998). Redox-dependent gene regulation in *Rhodobacter sphaeroides* 2.4.1^T: effects on dimethyl sulfoxide reductase (*dor*) gene expression. *J. Bacteriol.* 180, 5612–5618. doi: 10.1128/JB.180.21.5612-5618.1998

Murdeshwar, M. S., and Chatterji, D. (2012). MS_RHII-RSD, a dual-function RNase HII-(p)ppGpp synthetase from *Mycobacterium smegmatis*. *J. Bacteriol.* 194, 4003–4014. doi: 10.1128/JB.00258-12

Oh, J. I., and Kaplan, S. (1999). The cbb_3 terminal oxidase of *Rhodobacter sphaeroides* 2.4.1: structural and functional implications for the regulation of spectral complex formation. *Biochemistry* 38, 2688–2696. doi: 10.1021/bi9825100

Oh, Y., Lee, H. I., Jeong, J. A., Kim, S., and Oh, J. I. (2022). Activation of the SigE-SigB signaling pathway by inhibition of the respiratory electron transport chain and its effect on rifampicin resistance in *Mycobacterium smegmatis*. *J. Microbiol.* 60, 935–947. doi: 10.1007/s12275-022-2202-0

Oh, Y., and Oh, J. I. (2024). The RsfSR two-component system regulates SigF function by monitoring the state of the respiratory electron transport chain in *Mycobacterium smegmatis*. *J. Biol. Chem.* 300:105764. doi: 10.1016/j.jbc.2024.105764

Oh, J. I., Park, S. J., Shin, S. J., Ko, I. J., Han, S. J., Park, S. W., et al. (2010). Identification of *trans*- and *cis*-control elements involved in regulation of the carbon monoxide dehydrogenase genes in *Mycobacterium* sp. strain JC1 DSM 3803. *J. Bacteriol.* 192, 3925–3933. doi: 10.1128/JB.00286-10

Oh, Y., Song, S. Y., Kim, H. J., Han, G., Hwang, J., Kang, H. Y., et al. (2020). The partner switching system of the SigF sigma factor in *Mycobacterium smegmatis* and induction of the SigF regulon under respiration-inhibitory conditions. *Front. Microbiol.* 11:588487. doi: 10.3389/fmicb.2020.588487

Pang, X., Vu, P., Byrd, T. F., Ghanny, S., Soteropoulos, P., Mukamolova, G. V., et al. (2007). Evidance for complex interactions of stress-associated regulons in an *mprAB*

deletion mutant of *Mycobacterium tuberculosis*. *Microbiology* 153, 1229–1242. doi: 10.1099/mic.0.29281-0

Petchiappan, A., Naik, S. Y., and Chatterji, D. (2020). RelZ-mediated stress response in *Mycobacterium smegmatis*: pGpp synthesis and its regulation. *J. Bacteriol.* 202, e00444–19. doi: 10.1128/JB.00444-19

Primm, T. P., Andersen, S. J., Mizrahi, V., Avarbock, D., Rubin, H., and Barry, C. E. (2000). The stringent response of *Mycobacterium tuberculosis* is required for long-term survival. *J. Bacteriol.* 182, 4889–4898. doi: 10.1128/jb.182.17.4889-4898.2000

Prusa, J., Zhu, D. X., and Stallings, C. L. (2018). The stringent response and *Mycobacterium tuberculosis* pathogenesis. *Pathog. Dis.* 76:fty054. doi: 10.1093/femspd/fty054

Puustinen, A., Finel, M., Haltia, T., Gennis, R. B., and Wikstrom, M. (1991). Properties of the two terminal oxidases of *Escherichia coli*. *Biochemistry* 30, 3936–3942. doi: 10.1021/bi00230a019

Rifat, D., Bishai, W. R., and Karakousis, P. C. (2009). Phosphate depletion: a novel trigger for *Mycobacterium tuberculosis* persistence. *J. Infect. Dis.* 200, 1126–1135. doi: 10.1086/605700

Sanyal, S., Banerjee, S. K., Banerjee, R., Mukhopadhyay, J., and Kundu, M. (2013). Polyphosphate kinase 1, a central node in the stress response network of *Mycobacterium tuberculosis*, connects the two-component systems MprAB and SenX3-RegX3 and the extracytoplasmic function sigma factor, sigma E. *Microbiology* 159, 2074–2086. doi: 10.1099/mic.0.068452-0

Sherman, B. T., Hao, M., Qiu, J., Jiao, X., Baseler, M. W., Lane, H. C., et al. (2022). DAVID: a web server for functional enrichment analysis and functional annotation of gene lists (2021 update). *Nucleic Acids Res.* 50, W216–W221. doi: 10.1093/nar/gkac194

Shin, D. M., Jeon, B. Y., Lee, H. M., Jin, H. S., Yuk, J. M., Song, C. H., et al. (2010). *Mycobacterium tuberculosis* Eis regulates autophagy, inflammation, and cell death through redox-dependent signaling. *PLoS Pathog.* 6:e1001230. doi: 10.1371/journal.ppat.1001230

Shin, J., Singal, B., Gruber, A., Wong, D. M. K., Ragunathan, P., and Gruber, G. (2021a). Atomic structure of the regulatory TGS domain of Rel protein from *Mycobacteirum tuberculosis* and its interaction with deacylated tRNA. *FEBS Lett.* 595, 3006–3018. doi: 10.1002/1873-3468.14236

Shin, J., Singal, B., Manimekalai, M. S. S., Wei Chen, M., Ragunathan, P., and Grüber, G. (2021b). Atomic structure of, and valine binding to the regulatory ACT domain of the *Mycobacterium tuberculosis* Rel protein. *FEBS J.* 288, 2377–2397. doi: 10.1111/febs.15600

Singal, B., Balakrishna, A. M., Nartey, W., Manimekalai, M. S. S., Jeyakanthan, J., and Gruber, G. (2017). Crystallographic and solution structure of the N-terminal domain of the Rel protein from *Mycobacterium tuberculosis*. *FEBS Lett.* 591, 2323–2337. doi: 10.1002/1873-3468.12739

Snapper, S. B., Melton, R. E., Mustafa, S., Kieser, T., and Jacobs, W. R. (1990). Isolation and characterization of efficient plasmid transformation mutants of *Mycobacterium smegmatis*. *Mol. Microbiol.* 4, 1911–1919. doi: 10.1111/j.1365-2958.1990.tb02040.x

Stallings, C. L., Stephanou, N. C., Chu, L., Hochschild, A., Nickels, B. E., and Glickman, M. S. (2009). CarD is an essential regulator of rRNA transcription required for *Mycobacterium tuberculosis* persistence. *Cell* 138, 146–159. doi: 10.1016/j.cell.2009.04.041

Stover, S. L., Lloyd, L. K., Waites, K. B., and Jackson, A. B. (1991). Neurogenic urinary tract infection. *Neurol. Clin.* 9, 741–755. doi: 10.1016/S0733-8619(18)30277-9

Sureka, K., Dey, S., Datta, P., Singh, A. K., Dasgupta, A., Rodrigue, S., et al. (2007). Polyphosphate kinase is involved in stress-induced *mprAB-sigE-rel* signalling in mycobacteria. *Mol. Microbiol.* 65, 261–276. doi: 10.1111/j.1365-2958.2007.05814.x

Timm, J., Post, F. A., Bekker, L. G., Walther, G. B., Wainwright, H. C., Manganelli, R., et al. (2003). Differential expression of iron-, carbon-, and oxygen-responsive mycobacterial genes in the lungs of chronically infected mice and tuberculosis patients. *Proc. Natl. Acad. Sci. USA* 100, 14321–14326. doi: 10.1073/pnas.2436197100

Weiss, L. A., and Stallings, C. L. (2013). Essential roles for *Mycobacterium tuberculosis* Rel beyond the production of (p)ppGppG. *J. Bacteriol.* 195, 5629–5638. doi: 10.1128/jb.00759-13

White, M. J., He, H., Penoske, R. M., Twining, S. S., and Zahrt, T. C. (2010). PepD participates in the mycobacterial stress response mediated through MprAB and SigE. *J. Bacteriol.* 192, 1498–1510. doi: 10.1128/JB.01167-09

Wiseman, B., Nitharwal, R. G., Fedotovskaya, O., Schafer, J., Guo, H., Kuang, Q., et al. (2018). Structure of a functional obligate complex III₂IV₂ respiratory supercomplex from *Mycobacterium smegmatis*. *Nat. Struct. Mol. Biol.* 25, 1128–1136. doi: 10.1038/s41594-018-0160-3

Wu, M. L., Gengenbacher, M., Chung, J. C., Chen, S. L., Mollenkopf, H. J., Kaufmann, S. H., et al. (2016). Developmental transcriptome of resting cell formation in *Mycobacterium smegmatis*. *BMC Genomics* 17:837. doi: 10.1186/s12864-016-3190-4

Yanisch-Perron, C., Vieira, J., and Messing, J. (1985). Improved M13 phage cloning vectors and host strains: nucleotide sequences of the M13mp18 and pUC19 vectors. *Gene* 33, 103–119. doi: 10.1016/0378-1119(85)90120-9

Zahrt, T. C. (2003). Molecular mechanisms regulating persistent *Mycobacterium tuberculosis* infection. *Microbes Infect.* 5, 159–167. doi: 10.1016/s1286-4579(02)00083-7

Zahrt, T. C., and Deretic, V. (2001). *Mycobacterium tuberculosis* signal transduction system required for persistent infections. *Proc. Natl. Acad. Sci. USA* 98, 12706–12711. doi: 10.1073/pnas.221272198

Zhou, S., Wang, W., Zhou, X., Zhang, Y., Lai, Y., Tang, Y., et al. (2021). Structure of *Mycobacterium tuberculosis* cytochrome *bcc* in complex with Q203 and TB47, two anti-TB drug candidates. *eLife* 10:e69418. doi: 10.7554/eLife.69418